Prediction Of Worldwide Energy Resource (POWER)
--- Sustainable Buildings Methodology ---
(0.5^{o} Latitude by 0.5^{o} Longitude Spatial Resolution)

(Version 1.0 May 14, 2015)

Paul W. Stackhouse, Jr[1], David Westberg[2], James M. Hoell[2], William S. Chandler[2], Taiping Zhang[2]
[1]NASA Langley Research Center [2]SSAI/NASA Langley Research Center

Contents

1. Introduction **1**

2. Parameters & Data Sources **2**

3. Summary Of Parameter Accuracy **3**
3.1. **Solar Insolation** **3**
3.2 **Meteorology** **5**

4. **Global Insolation on a Horizontal Surface** 7
4.1 **Earth's Radiation Budget** **8**
4.2 Radiative Transfer Models **9**
4.2.1 **GEWEX SRB 3.0 Radiative Transfer Model** **9**
4.2.2 **FLASHFlux Radiative Transfer Model** **10**
4.3 **Validation:** **11**
4.3.1 SRB 3.0 Solar Insolation 12
4.3.1.1 **SW Daily Mean All Sky Conditions**..... **12**
4.3.1.2 **LW Daily Mean All Sky Conditions** **14**
4.3.1.3 **SW Daily Mean Clear Sky Conditions** **15**
4.3. 2 FLASHFlux Solar Insolation 17
4.3.2.1 **SW Daily Mean: FLASHFlux Versions 2H, 3A, and 2H+3A**.... **18**
4.3.2.2 **LW Daily Mean: FLASHFlux Versions 2H, 3A, and 2H+3A**.... **20**

5. Meteorological Parameters **24**
5.1 **Maximum, Minimum, & Average Temperatures** **25**
5.2 **Relative Humidity** **30**
5.3 **Dew/Frost Point Temperatures** **33**
5.4 **Precipitation** **35**
5.5 **Wind Speed Parameters** **39**
5.6 **Heating/Cooling Degree Days** **40**
5.7 **Surface Pressure** **42**

6. References **44**

1. Introduction

NASA, through its' Earth science research program has long supported satellite systems and research providing data important to the study of climate and climate processes. These data include long-term estimates of meteorological quantities and surface solar energy fluxes. These satellite and modeled based products have also been shown to be accurate enough to provide reliable solar and meteorological resource data over regions where surface measurements are sparse or nonexistent, and offer two unique features – the data is global and, in general, contiguous in time. These two important characteristics, however, tend to generate very large data files/archives which can be intimidating for users, particularly those with little experience or resources to explore these large data sets. Moreover, the data products contained in the various NASA archives are often in formats that present challenges to new users. NASA's Applied Sciences Program (http://science.nasa.gov/earth-science/applied-sciences/) was established to foster the use of Earth science research results for near-term applications and benefits. The Prediction Of Worldwide Energy Resource (POWER) project is one of the activities funded by the Applied Science Program.

The POWER project was initiated in 2003 as an outgrowth of the Surface meteorology and Solar Energy (SSE - https://eosweb.larc.nasa.gov/project/sse/sse_table) project. The SSE project has as its focus the development of parameters related to the solar based energy industry. The current POWER project encompasses the SSE project with the objective to improve subsequent releases of SSE, and to create new datasets with applicability to the architectural (e.g. Sustainable buildings) and agricultural (e.g. Agro-climatology) industries. The POWER web interface (http://power.larc.nasa.gov) currently provides a portal to the SSE data archive, tailored for the renewable energy industry, as well as to the Sustainable Buildings Archive with parameters tailored for the sustainable buildings community, and the Agro-climatology Archive with parameters for the agricultural industry. In general, the underlying data behind the parameters used by each of these industries is the same – global solar radiation, or insolation, and meteorology, including surface and air temperatures, moisture, and winds.

The purpose of this document is to describe the underlying data contained in the Sustainable Buildings Archive, and to provide additional information relative to the various industry specific parameters, their limitations, and estimated accuracies. The intent is to provide information that will enable new and/or long time users to make decisions concerning the suitability of the Sustainable Buildings data for their particular project. This document is focused primarily on the Sustainable Buildings parameters, and in particular parameters derived from NASA data having a spatial resolution of 0.5^{o} latitude by 0.5^{o} longitude.

Companion documents describe the data and parameters in the POWER/SSE and POWER/Agro-climatology sections of the POWER data portal.

(Return to Content)

2. Parameters & Data Sources:

The parameters contained in the Sustainable Buildings Archive are based primarily upon solar radiation derived from satellite observations and meteorological data from assimilation models. The various parameters have been selected and developed through close collaboration with industry and government partners in the buildings community, and a web-based portal provides access to these industry-friendly parameters.

The archive contains:

Solar Insolation and Meteorology;

(1) Daily averaged solar insolation from July 1, 1983 to within several months of real time;
(2) Daily averaged air pressure, humidity, dew point temperature, wind speed & relative humidity and daily max and minimum temperatures from January 1, 1981 to within several months of real-time;

Department of Energy (DOE)/ASHRAE Building Climate Parameters on a global 0.5^o latitude/longitude grid including:

(1) Monthly averaged temperatures, precipitation , and heating & cooling degree days by year from January 1981 – December 2011
(2) Yearly average climate type (e.g. dry, humid , marine) and zone by year from 1981 - 2011

The parameters enumerated above are available globally on a user specified 0.5^o -degree latitude/longitude grid and represent the average value over the respective grid. Solar parameters in the Sustainable Buildings Archive are based upon an array of satellite observations which provide global estimates of the surface and top-of-atmosphere irradiance.

(1) For the time period July 1, 1983 – December 31, 2007 the solar parameters are based upon data from release 3 of the NASA/GEWEX Surface Radiation Budget project (GEWEX SRB 3.0 - http://gewex-srb.larc.nasa.gov/ & https://eosweb.larc.nasa.gov/project/srb/srb_table);
(2) For the time period January 1, 2008 to December 31, 2012 the solar parameters are based upon data from NASA's Fast Longwave And SHortwave Radiative Fluxes (FLASHFlux - http://flashflux.larc.nasa.gov/) project version-2H ; and FLASHFlux version-3A from January 1, 2013 to within a week of real time. For a discussion of the differences between the various versions of FLASHFlux the User is referred to https://eosweb.larc.nasa.gov/sites/default/files/project/ceres/quality_summaries/FFv3_TISA_DQS.pdf , section "Data Sets within the Version3 family."

The solar data from these primary sources are produced on a global 1° latitude/ longitude grid and replicated to a 0.5^o spatial grid via replication of the 1° values to the four 0.5^o grid cells within the respective 1° cell.

Note that the time series of daily surface insolation are comprised of values from the GEWEX SRB project (July 1983 – December 31 2007) and the FLASHFlux project versions-2H & -3A (January 1, 2008 – near real time). Accordingly, care should be taken when assessing climate trends that encompass changes in the versions of the solar data.

Meteorological parameters are taken from NASA's Modern Era Retro-analysis for Research and Applications – (MERRA) assimilation model (http://gmao.gsfc.nasa.gov/merra/) and the GEOS-5 Forward Processing for Instrument Teams (FP-IT) assimilation model. Both MERRA and FP-IT are major new versions of NASA's Goddard Earth Observing System Data Assimilation System Version 5 [GEOS-5; Rienecker et al. (2008, 2011) and Molod et al. (2011)]. Values from each model are initially produced on a 1/2-degree by 2/3-degree global grid and then bi-linearly interpolated by the POWER project to a global 0.5^{o} grid. The data are also transformed from Universal Time (UT) to solar local time (i.e., noon is defined to be solar noon without local time zone definitions taken into account). The MERRA meteorological data encompasses the time period from January 1, 1981 through approximately three months before current time; the values from the FP-IT assimilation model is appended to the MERRA data stream for the current time minus approximately three months through a few days before current time. Accordingly the combined meteorological time series spans the time period from 1981 through several day before current time. These models are identical at the core and therefore discontinuities as a result of concatenation of the data products should be minimal.

(Return to Content)

3. Summary of Parameters Accuracy: This section provides a summary of the estimated uncertainty associated with the data underlying the solar and metrological parameters available through the POWER/Sustainable Buildings Archive. The uncertainty estimates are based upon comparisons with surface measurements. A more detailed description of the parameters and the procedures used to estimate their uncertainties is given in the subsequent sections of this document.

3.1 Solar Insolation: Quality surface-measurements are generally considered more accurate than satellite-derived values. However, measurement uncertainties from calibration drift, operational uncertainties, instrumental changes, or data gaps are often unknown or unreported for many surface data sets. In 1989, the World Climate Research Program estimated "end-to-end" uncertainties for most routinely-operation solar-radiation ground sites in the range from 6 to 12%. Specialized high quality research sites such as those in the Baseline Surface Radiation Network (BSRN) are estimated to be more accurate by a factor of two. Note that the time series of daily insolation data available from the POWER archive are taken from the GEWEX SRB project (July 1983 – December 31 2007) and the FLASHFlux project versions -2H (January 1, 2008 – December 31, 2012) and -3A (January 1, 2013 – near real time). Accordingly, care should be taken when assessing climate trends that encompass changes in the source data.

The solar data from each project enumerated above were initially produced on a 1° latitude/longitude grid and subsequently re-gridded via data replication to a 0.5^{o} grid. The comparison of the satellite based values to surface observations was performed using the 1degree

gridded values. However, since the re-gridding to 0.5° was based upon replication of values, the 1° comparison results are applicable to the 0.5° data.

Table 3.1.1 summarizes the results of comparing the NASA/GEWEX SRB 3.0 solar shortwave (SW), longwave (LW), and clear sky SW insolation on a horizontal surface to observations obtained at 47 BSRN stations (see Figure 4.3.1).

3.1.1 Comparisons of all sky shortwave (SW) and longwave (LW) solar insolation from NASA/GEWEX SRB 3.0 versus BSRN (Figure 4.3.1) insolation on a horizontal surface for the time period January 1, 1992 - December 31, 2007

Parameter	Region: All BSRN Sites	Bias (%)	RMSE (%)
Daily Mean SW All Sky Insolation NASA/GEWEX SRB 3.0 (Figure 4.3.1.1.1)	Global 60° Poleward 60° Equatorward	-1.72 -6.94 -1.13	20.47 41.59 17.66
Daily Mean LW All Sky Insolation NASA/GEWEX SRB 3.0 (Figure 4.3.1.2.1)	Global 60° Poleward 60° Equatorward	0.16 1.27 -0.03	7.0 13.44 5.73
Daily Mean SW Clear Sky Insolation (Figure 4.3.1.3.2)	Global	-0.84	7.04

Tables 3.1.2 and 3.1.3 summarize respectively the comparison of the FLASHFLux solar SW and LW insolation to 59 BSRN observational sites **(Figure 4.3.2.)**.

Table 3.1.2: Comparison of all sky shortwave (SW) solar insolation from FLASHFlux versions -2H, -3A, and for 2H + 3A versus observations from 59 BSRN ground sites (Figure 4.3.2) for the time period January 1, 2008 – July, 2013.

Parameter	Region: All BSRN Sites	Bias (%)	RMSE (%)
Daily Mean All Sky SW Insolation FLASHFlux Version 2H Jan.1, 2008 – Dec.31, 2012 (Figure 4.3.2.1.1)	Global 60° Poleward 60° Equatorward	0.02 -5.54 0.67	17.54 34.56 14.76
Daily Mean All Sky SW Insolation FLASHFlux Version 3A Jan.1, 2013 – Sep. 30, 2013 (Figure 4.3.2.1.2)	Global 60° Poleward 60° Equatorward	-5.43 -6.26 -5.37	20.02 38.92 18.06
Daily Mean All Sky SW Insolation FLASHFlux Version 2H + 3A Jan.1, 2008 – Sep. 30, 2013 (Figure 4.3.2.1.3)	Global 60° Poleward 60° Equatorward	-0.36 -5.58 0.24	17.73 34.79 15.03

Table 3.1.3.: Comparison of longwave (LW) solar insolation from FLASHFlux versions -2H, -3A, and for 2H + 3A versus BSRN (Figure 4.3.2.) insolation on a horizontal surface for the time period January 1, 2008 – July, 2013

Parameter	Region: All BSRN Sites	Bias (%)	RMSE (%)
Daily Mean LW All Sky Insolation FLASHFlux Version 2H Jan. 1, 2008 – Dec. 31, 2012 (Figure 4.3.2.2.1)	Global 60° Poleward 60° Equatorward	-0.29 0.79 -0.45	6.39 13.79 5.15
Daily Mean LW All Sky Insolation FLASHFlux Version 3A Jan. 1, 2013 – Sep. 30, 2013 (Figure 4.3.2.2.2)	Global 60° Poleward 60° Equatorward	0.63 3.93 0.32	7.98 9.48 7.78
Daily Mean LW All Sky Insolation FLASHFlux Version 2H + 3A Jan. 1, 2008 – Sep. 30, 2013 (Figure 4.3.2.2.3)	Global 60° Poleward 60° Equatorward	-0.24 0.92 -0.40	6.49 13.66 5.35

(Return to Content)

3.2 Meteorology This section provides a summary of the estimated uncertainty associated with the 0.5^{o} spatially resolved primary meteorological parameters (temperature, precipitation, winds, pressure, etc) available through the POWER/Sustainable Buildings Archive, as well as a comparison of parameters calculated (i.e. cooling & heating degree days, dew point, relative humidity, etc.) based upon the primary parameters. The uncertainty estimates are based upon comparisons with the corresponding parameters directly measured or calculated using surface observations.

Table 3.2.1 summarizes the results of comparing MERRA based meteorological parameters to those based upon globally distributed surface observations reported in the National Center for Environmental Information (NCEI – formally National Climatic Data Center) global summary of the day (GSOD) files. The slope, intercept, and R^2 listed in this table are associated with a linear least squares fit to a scatter plot of daily observations at each surface station to the corresponding MERRA values for the overlapping grid cell over all the indicated years. The Mean Bias Error (MBE) and Root Mean Square Error (RMSE) are also associated with all the indicated years.

Table 3.2.1: Listed in this Table are the climatologically averaged statistics associated with comparisons of the daily meteorological parameters from the MERRA assimilation model to corresponding values reported or calculated from surface observation in the National Center for Environmental Information (NCEI – formally National Climatic Data Center) GSOD files for the time period January 1, 1981 through December 31, 2012. The HDD & CDD statistics are for the time period January 1, 1981 through December 31, 2011.

Parameter	MBE	RMSE	Slope	Intercept	Rsqrd
Tavg (°C) (Table 5.1.1)	0.16	2.50	1.00	0.16	0.95
Tmin (°C) (Table 5.1.1)	0.95	3.44	0.98	1.11	0.92
Tmax (°C) (Table 5.1.1)	-0.72	3.28	0.99	-0.52	0.93
RH (%) (Table 5.2.2)	2.86	12.10	0.82	15.52	0.60
Tdew (°C) (Table 5.3.1)	0.64	2.83	0.95	0.93	0.93
Daily Precipitation (mm/day) (Table 3.4.2.1)	0.23	7.04	0.24	1.72	0.14
Wind Speed (m/s) (Table 5.5.1)	0.36	1.74	0.65	1.64	0.48
Heating Degree Days (degree days) (Figure V.F.1)	1.37	7.79	1.04	-8.53	0.99
Cooling Degree Days (degree days) (Figure 5.6.1)	6.73	9.13	1.04	0.29	0.99
Atmospheric Pressure (hPa) (Figure 5.7.1)	-0.09	2.93	1.00	1.48	1.00

Table 3.2.2. lists the climatologically averaged monthly Mean Bias Error (MBE) and Root Mean Square Error (RMSE) for the MERRA daily averaged temperature Tave, and the daily maximum (Tmax) and minimum (Tmin) temperatures with respective to the values taken from the National Center for Environmental Information (NCEI – formally National Climatic Data Center) GSOD files over the time period January 1, 1981 through December 31, 2012.

Table 3.2.2. Climatologically averaged monthly Mean Bias Error (MBE) and Root Mean Square Error (RMSE) of the daily MERRA temperatures with respect to corresponding values reported in the NCEI GSOD files over the time period January 1981 through December 31, 2012. All units in degrees C.

	JAN	FEB	MAR	APR	MAY	JUN	JUL	AUG	SEP	OCT	NOV	DEC	YR
Tave MBE	-0.32	-0.24	-0.12	0.09	0.33	0.44	0.56	0.64	0.55	0.23	-0.06	-0.22	0.15
Tave RMSE	3.05	2.80	2.55	2.39	2.30	2.28	2.32	2.31	2.18	2.16	2.51	2.97	2.48
Tmin MBE	0.54	0.56	0.60	0.78	0.96	1.05	1.20	1.38	1.40	1.22	0.99	0.74	0.93
Tmin RMSE	4.10	3.91	3.53	3.24	3.07	2.97	2.96	3.07	3.20	3.32	3.64	4.02	3.43
Tmax MBE	-1.29	-1.08	-0.89	-0.70	-0.50	-0.48	-0.37	-0.26	-0.30	-0.65	-1.03	-1.16	-0.78
Tmax RMSE	3.53	3.39	3.40	3.37	3.27	3.29	3.34	3.28	3.03	2.91	3.10	3.41	3.30

(Return to Content)

4. Global Insolation on a Horizontal Surface:

The daily mean solar radiation for the time period July 1983 – December 2007 are obtained from the NASA/Global Energy and Water Cycle Experiment - Surface Radiation Budget Project Release 3.0 archive (NASA/GEWEX SRB 3.0; see http://gewex-srb.larc.nasa.gov/ & https://eosweb.larc.nasa.gov/project/srb/srb_table). Daily Solar radiation for the time period from January 1, 2008 to December 31, 2012 is from version 2H of NASA's Fast Longwave And SHortwave Radiative Fluxes (FLASHFlux; see http://flashflux.larc.nasa.gov/) project and from FLASHFlus version 3A for the time period January 1, 2014 to within 1-week of current time.

The solar data from these primary sources are initially produced on a global 1° latitude/ longitude grid and translated to a 0.5^o spatial grid by the POWER project via replication of the 1° values to the four 0.5^o grid cells within the respective 1° cell. Validation of the satellite based values was conducted via comparisons to surface observations using the 1-degree gridded values. However, since the re-gridding to 0.5^o was based upon replication of values, the 1° comparison results are applicable to the 0.5^o data.

The NASA/GEWEX SRB Project focuses on providing estimates of the Earth's Top-of-atmosphere (TOA) and surface solar insolation in support of NASA's effort to quantify components of the Earth's radiation budget, while the focus of the FLASHFlux project is to provide solar data within one week of satellite observations.

While it is not the intent or purpose of this document to provide a detailed description of the methodology for inferring solar data from satellite observations, a brief synopsis is provided in the following sections. (Return to Content)

4.1 Earth's Radiation Budget*:* A central focus of the NASA's satellite programs is to quantify the process associated with the Earth's energy budget. Figure 4.1.1 illustrates the major components/processes associated with the Earth's Energy Budget including updated radiative flux components estimated from SRB Release 3.0 in the yellow boxes.

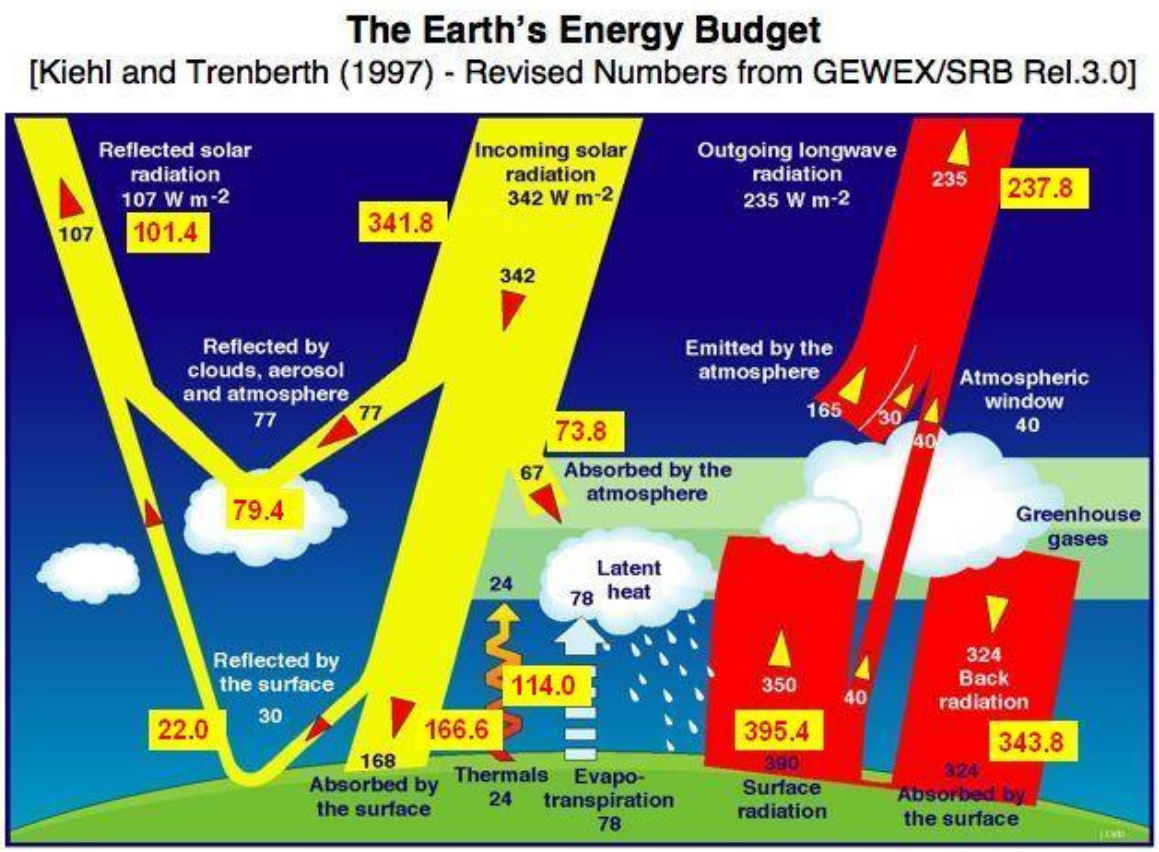

Figure 4.1.1. The major components/processes associated with the Earth's Energy Budget. The values in the yellow rectangles are based upon the updated solar and thermal infrared radiation estimates in SRB Release 3.0. (Note that all units are in W/m^2; multiplying W/m^2 by 0.024 yields kWh/day/m^2, and by 0.0864 yields MJ/day/m^2.)

These values are based on a 24 year (July 1983 – Dec. 2007) annual global averaged radiative fluxes with year-to-year annual average variability of +/- 4 W m^{-2} in the solar wavelengths and +/- 2 W m^{-2} in the thermal infrared (longwave) flux estimates. The absolute uncertainty of these components is still the subject of active research. For instances, the most recent satellite based measurements of the incoming solar radiation disagree with previous measurements and indicate this value should be closer 340.3 W m^{-2} providing another source of uncertainty. Other uncertainties involving the calibration of satellite radiances, atmospheric properties of clouds,

aerosols and gaseous constituents, surface spectral albedos are all the subject of research within the GEWEX SRB project.
(Return to Content)

4.2 Radiative Transfer Models: The surface solar insolation available from the POWER data archives is based upon observational data from a variety of satellites. The basic observational data is the amount of radiation emerging from the earth's atmosphere (see Fig. 4.1.1). The amount of radiation measured is affected by atmospheric absorption, emission and scattering processes. The radiative transfer equation mathematically describes these processes. In general, solar radiation is inferred from the satellite observations via an inversion of the radiative transfer equation.

4.2.1. GEWEX SRB Radiative Transfer Model*:* The modified method of Pinker and Laszlo (1992) is used to solve the radiative transfer equation and provided the GEWEX SRB 3.0 estimates of surface solar insolation. This method involves the use of a radiative transfer model, along with water vapor column amounts from the MERRA product and ozone column amounts from satellite measurements. Three satellite visible radiances are used: the instantaneous clear sky radiance, the instantaneous cloudy sky radiance, and the clear sky composite radiance, which is a representation of a recent dark background value. The observed satellite radiances are converted into broadband shortwave TOA albedos, using Angular Distribution Models from the Earth Radiation Budget Experiment (Smith et al., 1986). The spectral shape of the surface albedo is fixed by surface type. The radiative transfer model (through the use of lookup tables) is then used to find the absolute value of the surface albedo which produces a TOA upward flux which matches the TOA flux from the conversion of the clear-sky composite radiance. For this step, a first guess of the aerosol amount is used. The aerosol used for this purpose was derived from six years (2000-2005) of daily output from the MATCH chemical transport model (Rasch *et al.*,1997). A climatology of aerosol optical depth was developed for each of the twelve months by collecting the daily data for each grid cell, and finding the mode of the frequency distribution. The mode was used rather than the average so as to provide a typical background value of the aerosol, rather than an average which includes much higher episodic outbreak values. The surface albedo now being fixed, the aerosol optical depth is chosen within the radiative transfer model to produce a TOA flux which matches the TOA Flux from the conversion of the instantaneous clear sky radiance. Similarly the cloud optical depth is chosen to match the TOA flux implied from the instantaneous cloudy sky radiance. With all parameters now fixed, the model outputs a range of parameters including surface and TOA fluxes. All NASA/GEWEX SRB 3.0 parameters are output on a 1^0 by 1^0 global grid at 3-hourly temporal resolution for each day of the month.

Primary inputs to the model include: visible and infrared radiances, and cloud and surface properties inferred from International Satellite Cloud Climatology Project (ISCCP) pixel-level (DX) data (Rossow and Schiffer, 1999; data sets and additional information can be found at https://eosweb.larc.nasa.gov/project/isccp/isccp_table); temperature and moisture profiles from MERRA reanalysis product obtained from the NASA Global Modeling and Assimilation Office (GMAO; Bloom et al., 2005); and column ozone amounts constituted from Total Ozone Mapping Spectrometer (TOMS) and TIROS Operational Vertical Sounder (TOVS) archives, and

Stratospheric Monitoring-group's Ozone Blended Analysis (SMOBA), an assimilation product from NOAA's Climate Prediction Center.

To facilitate access to the GEWEX SRB 3.0 data products, the POWER project extracts the fundamental parameters (i.e. solar) from the SRB archive and metrological parameters from the GMAO assimilation models and precipitation from the GPCP archives. These data products are available through the POWER/Sustainable Building Archive.
(Return to Content)

4.2.2. FLASHFlux Radiative Transfer Model: The Fast Longwave and SHortwave Flux (FLASHFlux) project is based upon the algorithms developed for analysis and data collected by the Clouds and the Earth's Radiant Energy System (CERES - http://ceres.larc.nasa.gov/) project. CERES is currently producing world-class climate data products derived from measurements taken aboard NASA's Terra and Aqua spacecrafts. While of exceptional fidelity, CERES data products require a extensive calibration checks and validation to assure quality and verify accuracy and precision. The result is that CERES data are typically released more than six months after acquisition of the initial measurements. For climate studies, such delays are of little consequence especially considering the improved quality of the released data products. There are, however, many uses for the CERES data products on a near real-time basis such as those referred to within the POWER project. To meet those needs, FLASHFlux has greatly sped up the processing by using the earliest stream of data coming from CERES instruments and using fast radiation algorithms to produce results within one week of satellite observations. This results in the loss of climate-quality accuracy due to bypassing of some calibration checks, and some gaps in the earliest stream of satellite data.

For speedy retrieval of surface insolation, FLASHFlux uses the SW Model B that is also used in CERES processing. This model is named the Langley Parameterized SW Algorithm (LPSA) and described in detail in Gupta et al. (2001). It consists of physical parameterizations which account for the attenuation of solar radiation in simple terms separately for clear atmosphere and clouds. Surface insolation, F_{sd}, is computed as

4.2.2.1 $$F_{sd} = F_{toa} \; T_a \; T_c \,,$$

where F_{toa} is the corresponding TOA insolation, T_a is the transmittance of the clear atmosphere, and T_c is the transmittance of the clouds. Both FLASHFlux and CERES rely on similar input data sets from the meteorological products and Moderate Resolution Imaging Spectroradiometer (MODIS). However, it is important to note that even though the FLASHFlux endeavor intends to incorporate the latest input data sets and improvements into its algorithms, there are no plans to reprocess the FLASHFlux data products once these modifications are in place. Thus, in contrast to the CERES data products, the FLASHFlux data products are **not** to be considered of climate quality. Users seeking climate quality should instead use the CERES data products. In the following section estimates of the accuracy of the GEWEX SRB 3.0 and FLASHFlux solar data are provided.

For a discussion of the differences between the various versions of FLASHFlux the User is referred to
https://eosweb.larc.nasa.gov/sites/default/files/project/ceres/quality_summaries/FFv3_TISA_DQS.pdf , section “Data Sets within the Version3 family”

(Return to Content)

4.3. Validation: The GEWEX SRB and FLASHFlux radiative transfer models described in the preceding sections produce estimates of the solar insolation on a 1° latitude, longitude global grid. The validation of the SRB and FLASHFlux data is based on this 1° data. The 0.5^o spatial solar data in the POWER archive has been generated from the 1° data via a straight replication process that assigns the 1° grid value to each of the four 0.5^o grids contained in the respective 1° grid box. Consequently the validation results reported here and by White et. al. (2011) for the 1° values are applicable to the 0.5^o data.

Validation of both the SRB and FLASHFlux solar insolation is based upon comparisons against research quality observations from the Baseline Surface Radiation Network (BSRN; Ohmura *et al*., 1998). Figure 4.3.1 shows the location of 47 ground stations within the BSRN network used for the GEWEX SRB 3.0 validation. Figure 4.3.2 shows the location of 59 ground stations within the BSRN network used for the FLASHFlux validation.

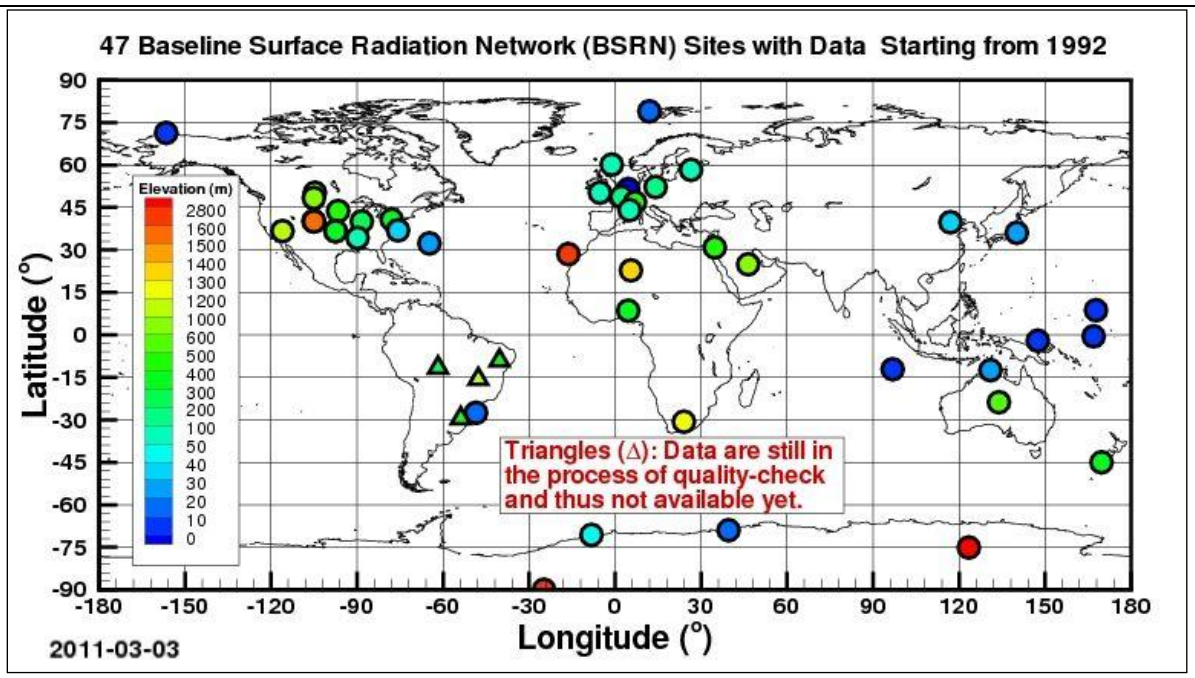

Figure 4.3.1. Location of ground stations in the Baseline Surface Radiation Network (BSRN). used for the validation of the SRB-3.0 insolation

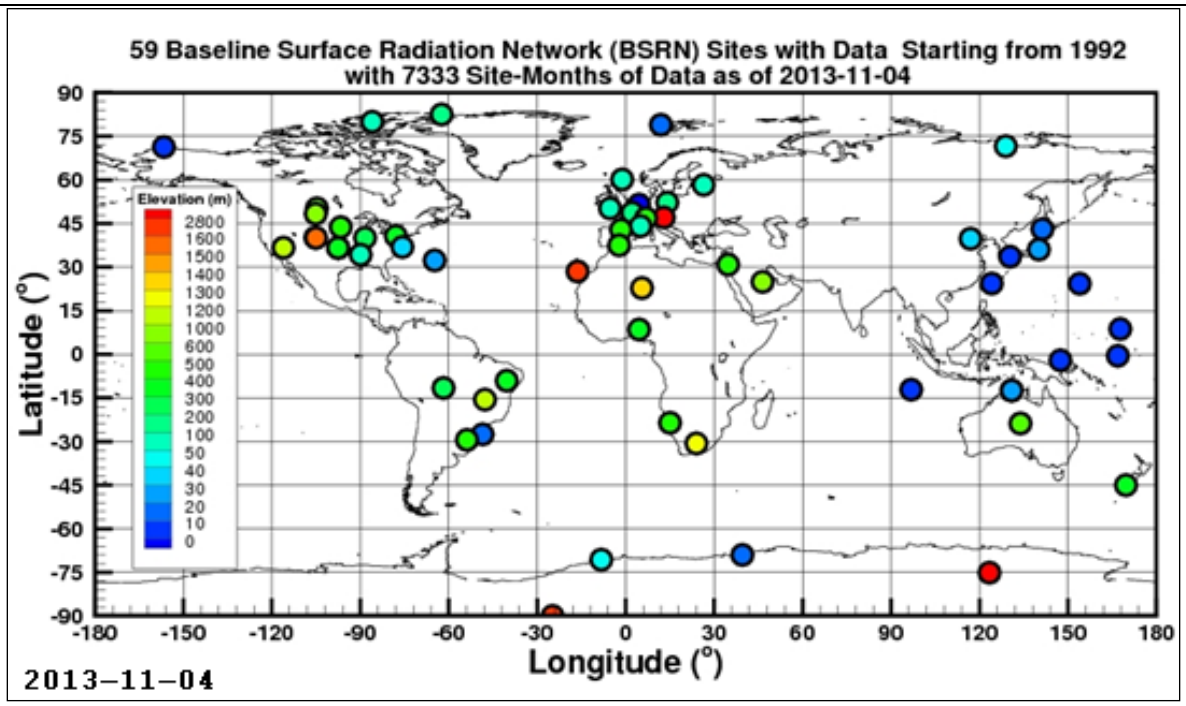

Figure 4.3.2. Location of ground stations in the Baseline Surface Radiation Network (BSRN) used to validation of the FLASHFlux solar insolation.

(Return to Content)

4.3.1. SRB 3.0 Solar Insolation The shortwave (SW) and longwave (LW) insolation values in the time period from July 1983 – December 2007 were taken from release 3 of the NASA/GEWEX Surface Radiation Budget project (GEWEX SRB 3.0 - http://gewex-srb.larc.nasa.gov/ & https://eosweb.larc.nasa.gov/project/srb/srb_table.

4.3.1.1 SRB 3.0 SW Daily Mean; Scatter plots of the total (i.e. diffuse plus direct) surface insolation observed at the BSRN ground sites versus the corresponding insolation values from the SRB release 3.0 archive are shown in Figure 4.3.1.1.1 for daily mean SW values. The comparison covers the time period January 1, 1992, the earliest that data from BSRN is available, through December 31, 2007. The statistics given in the upper left box are for all BSRN sites (Globally), those located 60-degree poleward, and for those located 60-degree equatorward. The Bias is the difference between the mean (μ) of the respective solar radiation values for SRB and BSRN. RMS is the root mean square difference between the respective SRB and BSRN values. The correlation coefficient between the SRB and BSRN values is given by ρ, the variance in the SRB values is given by σ, and N is number of SRB:BSRN month pairs for each latitude region.

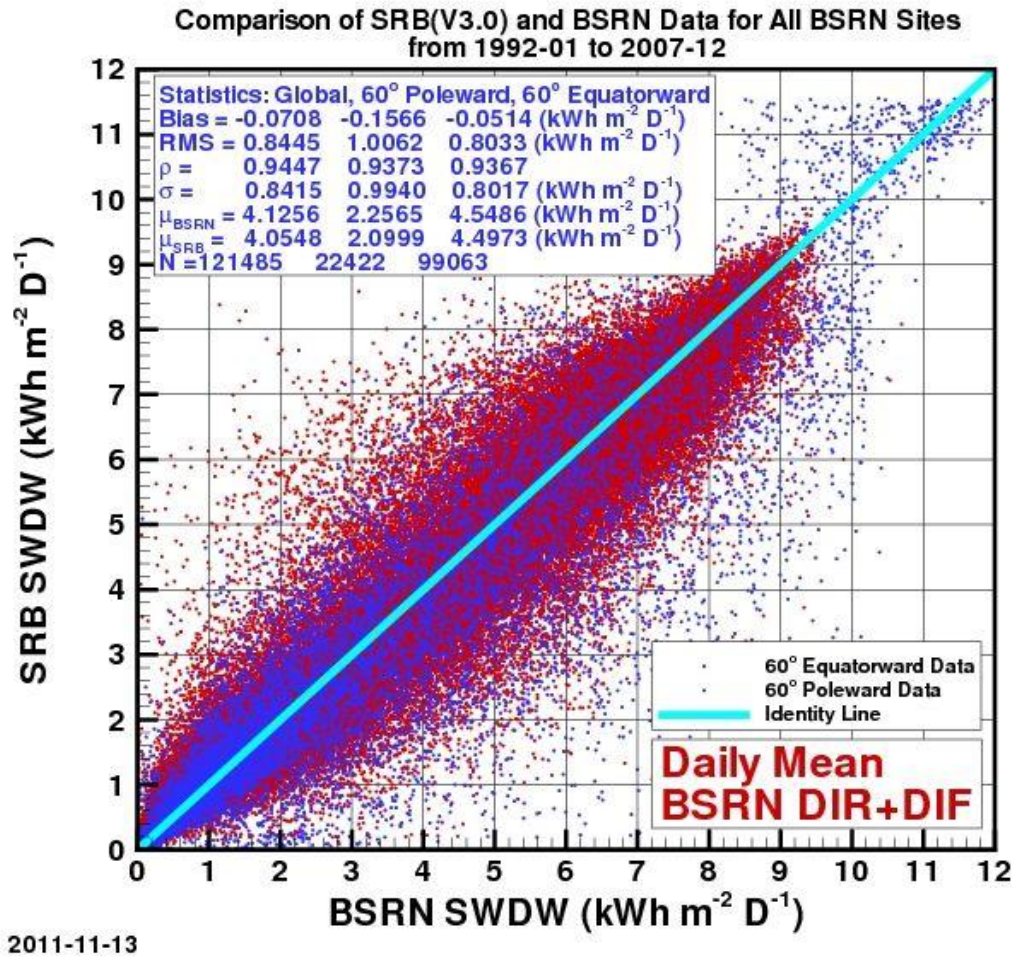

Figure 4.3.1.1.1. Scatter plot of daily total surface solar radiation observed at BSRN ground sites over the years 1992 - 2007 versus daily values from the GEWEX/SRB Release 3.0 archive all sky conditions. These daily are used to calculate the monthly averages that are provided in POWER/Sustainable Building Archive. The statistics given in the upper left box are for all BSRN sites (Globally), those located 60-degree poleward, and for those located 60-degree equatorward. The Bias is the difference between the mean (μ) of the respective solar radiation values for SRB and BSRN. RMS is the root mean square difference between the respective SRB and BSRN values. The correlation coefficient between the SRB and BSRN values is given by ρ, the variance in the SRB values is given by σ, and N is number of SRB:BSRN month pairs for each latitude region. (Note that the solar radiation unit is kWh/day/m^2; multiplying kWh/day/m^2 by 3.6 yields MJ/day/m^2, and by 41.67 yields W/m^2.)

Statistics from a comparison of the monthly climatological average of SRB V3 daily mean SW insolation to corresponding BSRN values over the time period from January 1, 1992 – December 31, 2007 are given in Table 4.3.1.1.1 along with the average over all the years.

Table 4.3.1.1.1 Statistics of SRB (V3.0)-BSRN daily mean shortwave downward flux comparison from 1992-01 to 2007-12.

Month	Bias (kWh/ m^2 da)	RMSE (kWh/ m^2 da)	ρ	M (kWh/ m^2 da)	Bias (%)	RMSE (%)	N
01	-0.096	0.8664	0.9449	3.1296	-3.09	27.68	9657
02	-0.0912	0.8232	0.9175	3.4536	-2.67	23.86	8781
03	-0.1152	0.8208	0.9207	3.9912	-2.87	20.59	10045
04	-0.0768	0.8064	0.9420	4.5144	-1.72	17.84	9947
05	-0.0648	0.8352	0.9489	5.0112	-1.29	16.67	10354
06	-0.0336	0.8952	0.9486	5.1408	-0.63	17.44	10217
07	0	0.84	0.9499	5.1264	0.01	16.38	10751
08	-0.036	0.7944	0.9428	4.7016	-0.78	16.88	10579
09	-0.0384	0.744	0.9351	4.248	-0.91	17.54	10149
10	-0.0768	0.8376	0.9171	3.6504	-2.09	22.92	10544
11	-0.1032	0.912	0.9273	3.1992	-3.21	28.52	10170
12	-0.1272	0.9384	0.9455	3.1368	-4.05	29.89	10291
Overall	**-0.072**	**0.8448**	**0.9447**	**4.1256**	**-1.72**	**20.47**	**121485**

.

(Return to Content)

4.3.1.2. SRB 3.0 LW Daily Mean: The longwave (LW) in the time period from July 1983 – December 2007 were taken from release 3 of the NASA/GEWEX Surface Radiation Budget project (GEWEX SRB 3.0 - http://gewex-srb.larc.nasa.gov/ & https://eosweb.larc.nasa.gov/project/srb/srb_table. A scatter plot of the daily mean LW surface insolation observed at the BSRN ground sites versus corresponding values from the SRB release 3.0 archive is shown in Figure 4.3.1.2.1. The comparisons cover the time period January 1, 1992, the earliest that data from BSRN is available, through December 31, 2007. The statistics given in the upper left box are for all BSRN sites (Globally), those located 60-degree poleward, and for those located 60-degree equatorward. The Bias is the difference between the mean (μ) of the respective solar radiation values for SRB and BSRN. RMS is the root mean square difference between the respective SRB and BSRN values. The correlation coefficient between the SRB and BSRN values is given by ρ, the variance in the SRB values is given by σ, and N is number of SRB:BSRN month pairs for each latitude region.

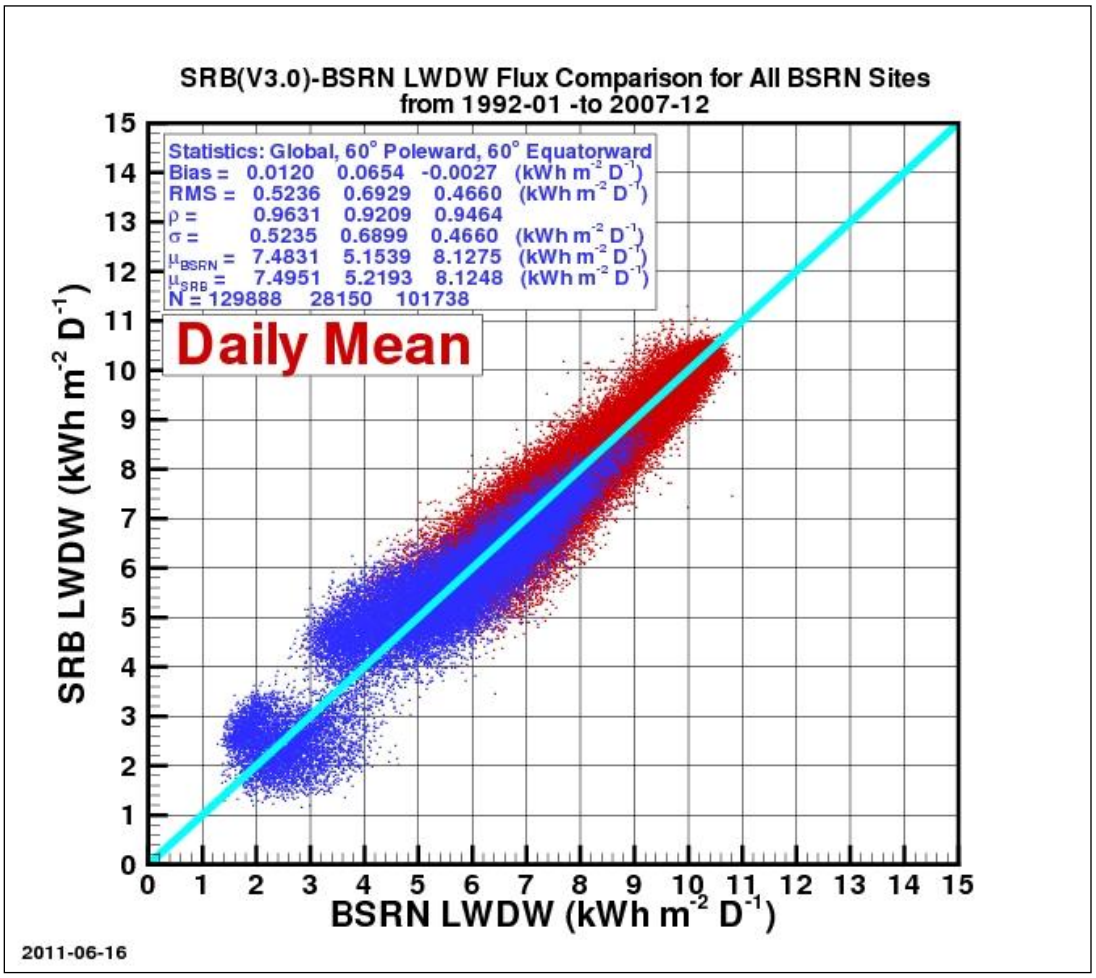

Figure 4.3.1.2.1. Scatter plot of daily mean total surface solar longwave insolation observed at BSRN ground sites over the years 1992 - 2007 versus daily means from the SRB Project for all sky conditions. The statistics given in the upper left box are for all BSRN sites (Globally), those located 60-degree poleward, and for those located 60-degree equatorward. The Bias is the difference between the mean (μ) of the respective solar radiation values for SRB and BSRN. RMS is the root mean square difference between the respective SRB and BSRN values. The correlation coefficient between the SRB and BSRN values is given by ρ, the variance in the SRB values is given by σ, and N is number of SRB:BSRN month pairs for each latitude region. (Note that the solar radiation unit is kWh/day/m^2; multiplying kWh/day/m^2 by 3.6 yields MJ/day/m^2, and by 41.67 yields W/m^2.)

(Return to Content)

4.3.1.3 SRB 3.0 Clear Sky Insolation: For these comparisons it was necessary to ensure that the ground observations and the satellite derived solar radiation values are for equivalent clear sky conditions. Fortunately, observational data from a number of BSRN ground sites (see Figure 4.3.1.3 .1) and the satellite observational data provide information related to cloud cover for each observational period. Cloud parameters from the NASA ISCCP were used to infer the solar

radiation in the GEWEX SRB 3.0 archive. Parameters within the ISCCP data provide a measure of the clearness for each satellite observation used in the SRB-inversion algorithms. Similarly, observations from upward viewing cameras at the 27 BSRN sites shown in Figure 4.3.1.3 .1provided a measure of cloud cover for each ground observational period. The comparison data shown in Figure 4.3.1.3 .2 used the ground cameras and the ISCCP data to match clearness conditions. In particular, the comparison shown below uses clearness criteria defined such that clouds in the field of view of the upward viewing camera and the field of view from the ISCCP satellites must both be less than 10%.

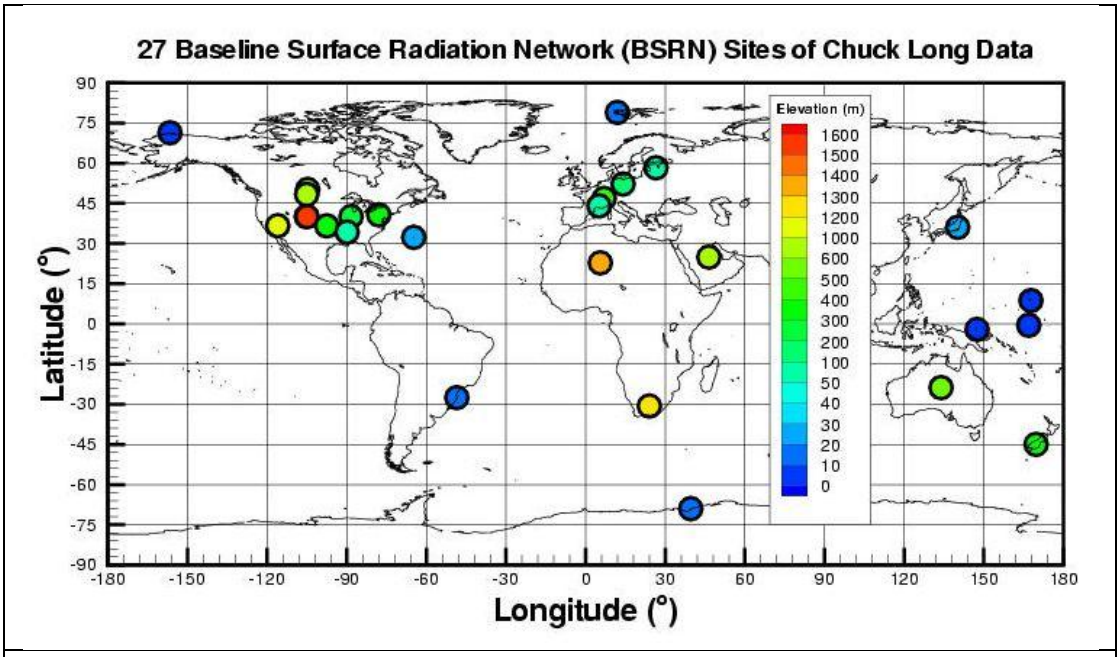

Figure 4.3.1.3 .1. Location of ground stations in the Baseline Surface Radiation Network (BSRN) with upward viewing cameras.

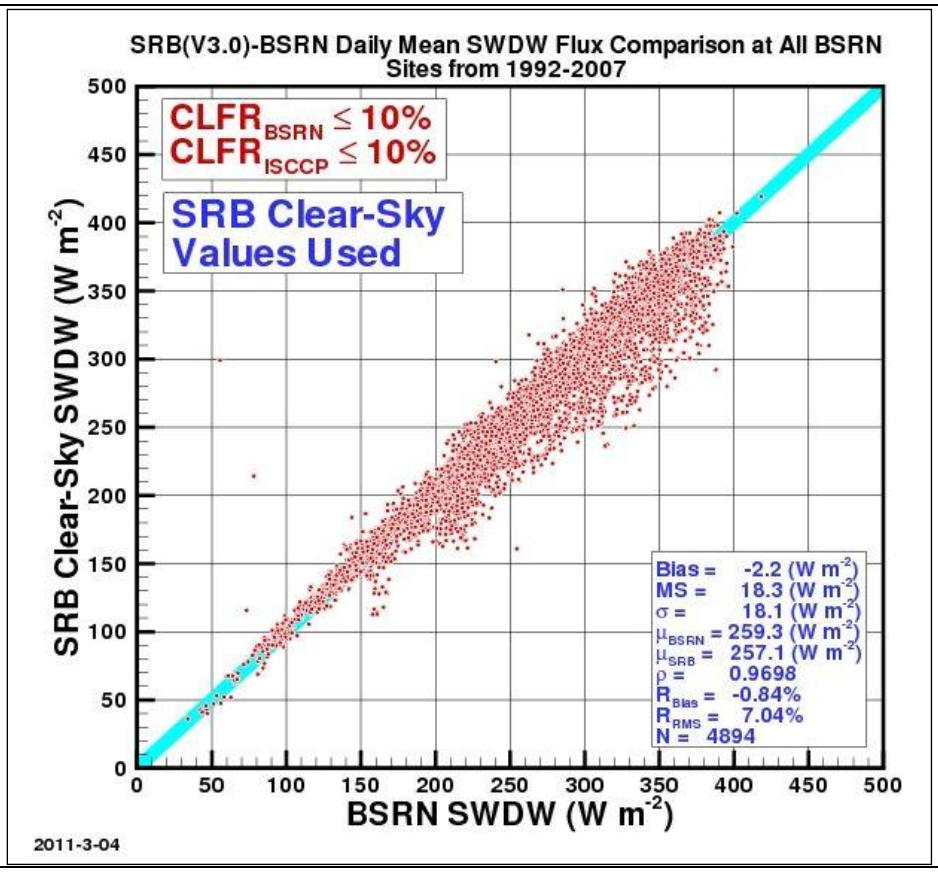

Figure 4.3.1.3.2. Scatter plot of the daily mean clear sky radiation derived from observations at BSRN ground sites vs. daily mean values from GEWEX SRB 3.0. Clear sky conditions are for less than 10% cloud cover in field-of-view of both the upward viewing ground and downward viewing satellite cameras. The Bias is the difference between the mean (μ) of the respective solar radiation values for SRB and BSRN. RMS is the root mean square difference between the respective SRB and BSRN values. The correlation coefficient between the SRB and BSRN values is given by ρ, the variance in the SRB values is given by σ, and N is number of SRB:BSRN month pairs for each latitude region. (Note that solar radiation is in W/m^2; multiplying W/m^2 by 0.024 yield KWh/m^2/day and by 0.0864 yields MJ/day/m^2.)

(Return to Content)

4.3.2. FLASHFlux: Beginning January 1, 2008, the SW and LW solar insolation values are taken from NASA's Fast Longwave And SHortwave Radiative Fluxes project (FLASHFlux - http://flashflux.larc.nasa.gov/) . For the time period January 1, 2008 to December 31, 2012 solar SW and LW values are based upon FLASHFlux version-2H ; and from January 1, 2013 to within a week of real time SW and LW values are from FLASHFlux version-3A. For a discussion of the differences between the various versions of FLASHFlux see https://eosweb.larc.nasa.gov/sites/default/files/project/ceres/quality_summaries/FFv3_TISA_DQS.pdf , section "Data Sets within the Version3 family."

4.3.2.1 . FLASHFlux Daily Mean SW; Scatter plots comparing the FLASHFlux SW solar data to the BSRN observations are shown in Figures 4.3.2.1.1, 4.3.2.1.2 and 4.3.2.1.3 for FLASHFlux versions -2H, -3A, and the ensemble of -2H plus -3A data respectively. The statistics given in the upper left box are for all BSRN sites (Globally), those located 60-degree poleward, and for those located 60-degree equatorward. The Bias is the difference between the mean (μ) of the respective solar radiation values for SRB and BSRN. RMS is the root mean square difference between the respective SRB and BSRN values. The correlation coefficient between the SRB and BSRN values is given by ρ, the variance in the SRB values is given by σ, and N is number of SRB:BSRN month pairs for each latitude region.

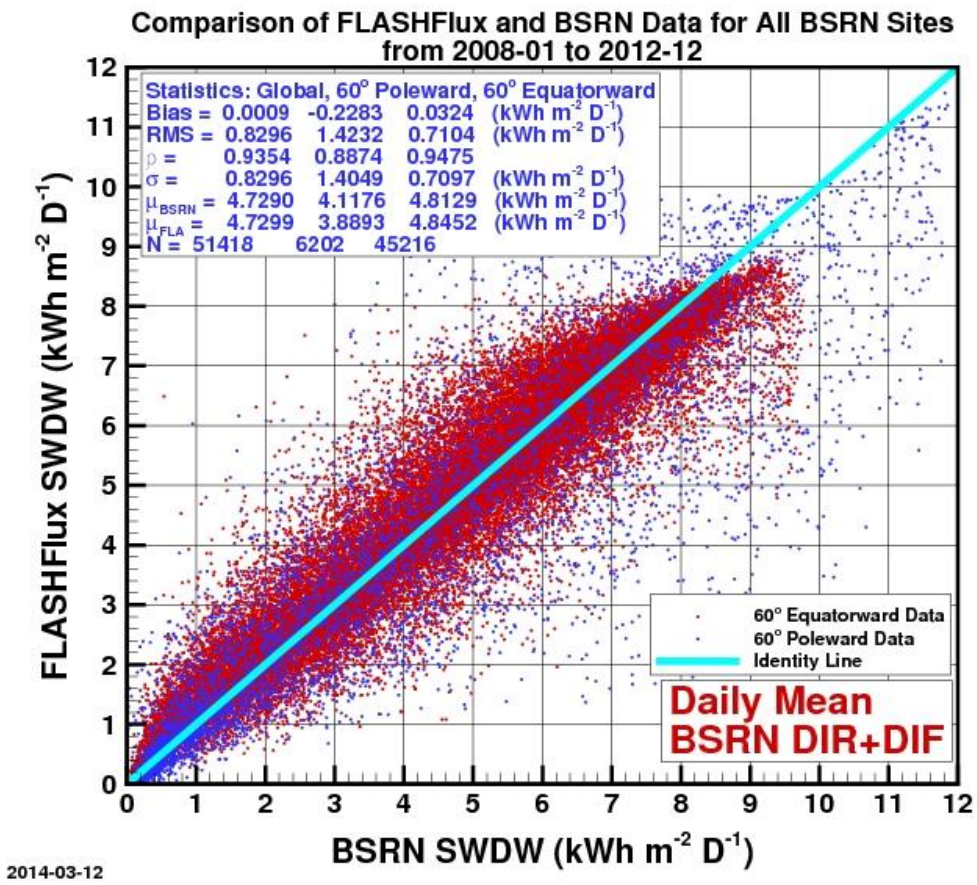

Figure 4.3.2.1.1. Scatter plot of daily total surface solar shortwave radiation observed at BSRN ground sites over the years January 1, 2008 – December 31, 2012 versus daily values from the FLASHFlux version 2H. The statistics given in the upper left box are for all BSRN sites (Globally), those located 60-degree poleward, and for those located 60-degree equatorward. The Bias is the difference between the mean (μ) of the respective solar radiation values for SRB and BSRN. RMS is the root mean square difference between the respective SRB and BSRN values. The correlation coefficient between the SRB and BSRN values is given by ρ, the variance in the SRB values is given by σ, and N is number of SRB:BSRN month pairs for each latitude region. (Note that the solar radiation unit is kWh/day/m^2; multiplying kWh/day/m^2 by 3.6 yields MJ/day/m^2, and by 41.67 yields W/m^2.)

(Return to Content)

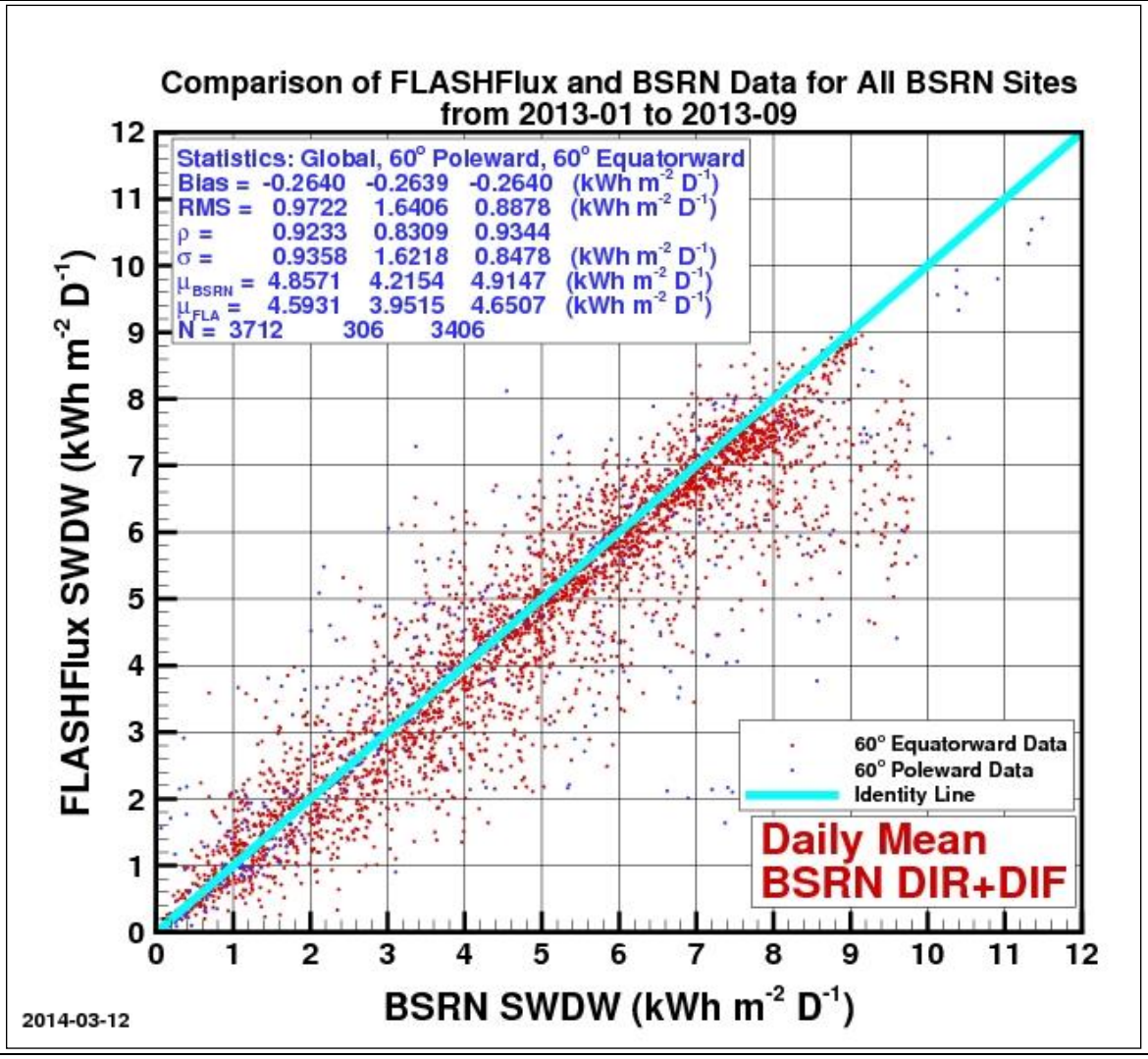

Figure 4.3.2.1.2. Scatter plot of daily total surface solar shortwave radiation observed at BSRN ground sites over the years January 1, 2013 – September 30, 2013 versus daily values from the FLASHFlux version 3A. The statistics given in the upper left box are for all BSRN sites (Globally), those located 60-degree poleward, and for those located 60-degree equatorward. The Bias is the difference between the mean (μ) of the respective solar radiation values for SRB and BSRN. RMS is the root mean square difference between the respective SRB and BSRN values. The correlation coefficient between the SRB and BSRN values is given by ρ, the variance in the SRB values is given by σ, and N is number of SRB:BSRN month pairs for each latitude region. (Note that the solar radiation unit is kWh/day/m^2; multiplying kWh/day/m^2 by 3.6 yields MJ/day/m^2, and by 41.67 yields W/m^2.)

(Return to Content)

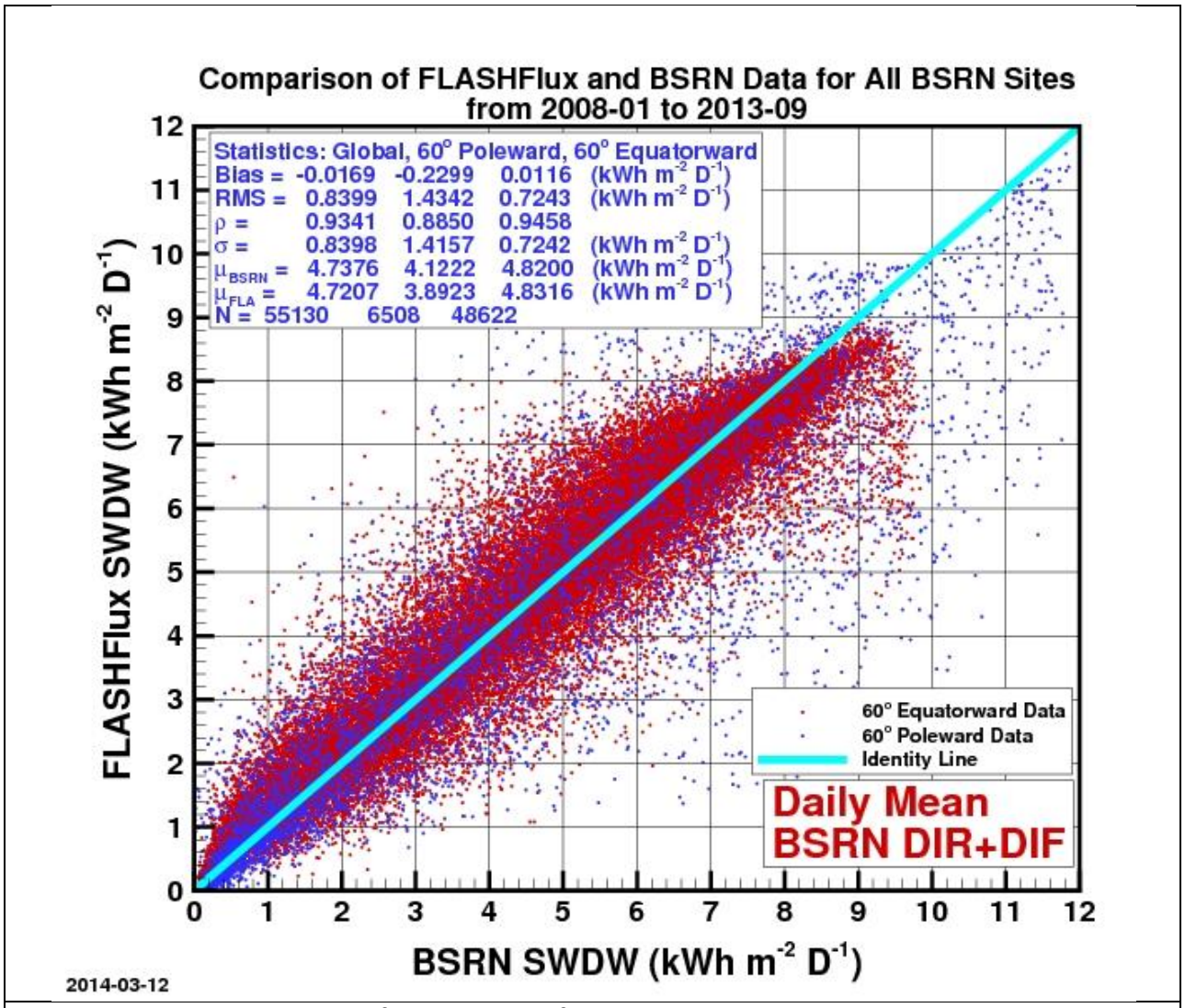

Figure 4.3.2.1.3. Scatter plot of daily total surface solar shortwave radiation observed at BSRN ground sites over the years January 1, 2008 – September 30, 2013 versus daily values from the FLASHFlux version 2H+3A. The statistics given in the upper left box are for all BSRN sites (Globally), those located 60-degree poleward, and for those located 60-degree equatorward. The Bias is the difference between the mean (μ) of the respective solar radiation values for SRB and BSRN. RMS is the root mean square difference between the respective SRB and BSRN values. The correlation coefficient between the SRB and BSRN values is given by ρ, the variance in the SRB values is given by σ, and N is number of SRB:BSRN month pairs for each latitude region. (Note that the solar radiation unit is kWh/day/m^2; multiplying kWh/day/m^2 by 3.6 yields MJ/day/m^2, and by 41.67 yields W/m^2.)

(Return to Content)

4.3.2.2. FLASHFlux Daily Mean LW: Scatter plots comparing the FLASHFlux LW solar data to the BSRN observations are shown in Figures 4.3.2.2.1, 4.3.2.2.2 and 4.3.2.2.3 for FLASHFlux versions -2H, -3A, and the ensemble of -2H plus -3A data respectively.

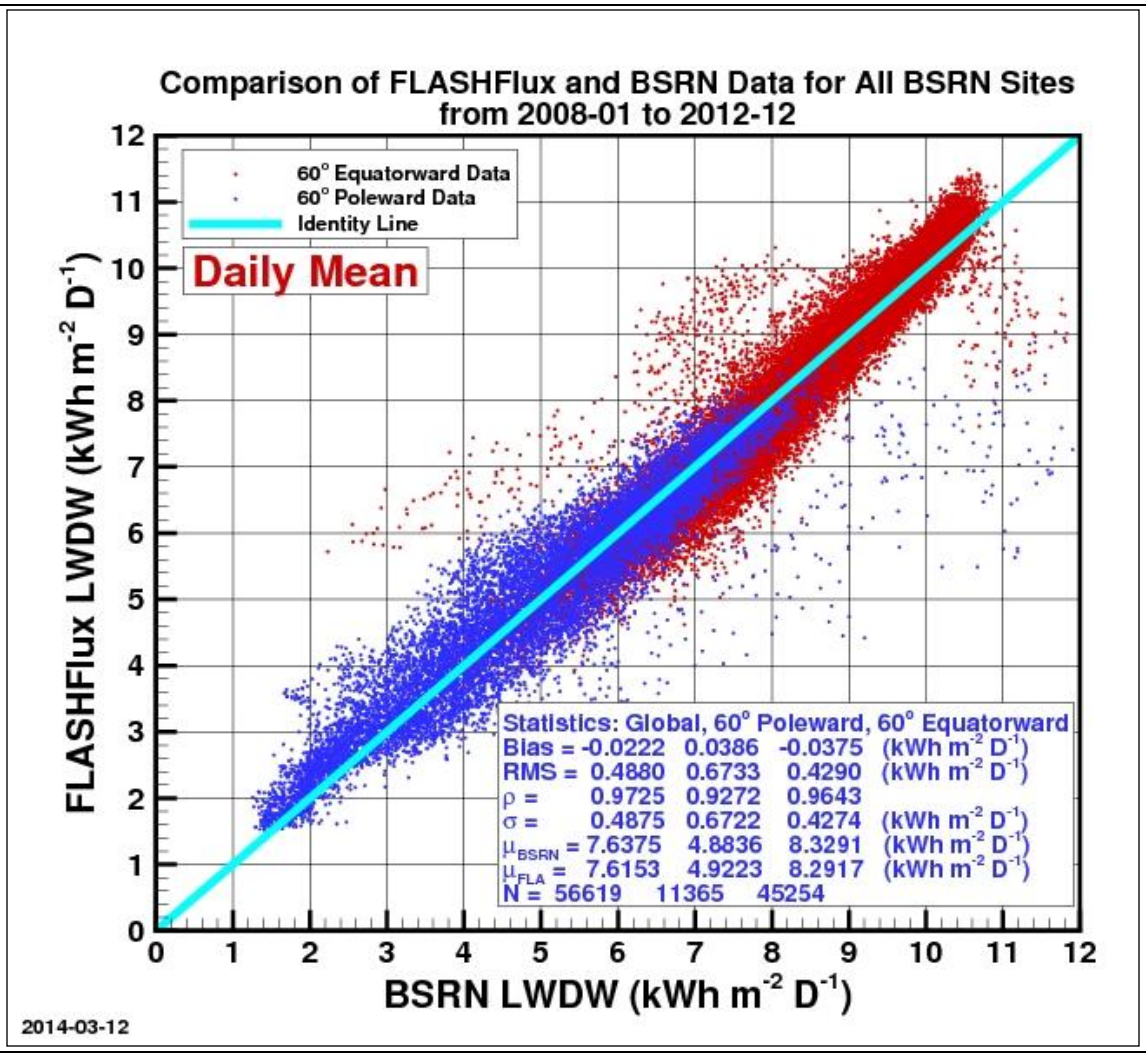

Figure 4.3.2.2.1. Scatter plot of daily total surface solar longwave radiation observed at BSRN ground sites over the years January, 2008 – December 31, 2012 versus daily values from the FLASHFlux version 2H. The statistics given in the upper left box are for all BSRN sites (Globally), those located 60-degree poleward, and for those located 60-degree equatorward. The Bias is the difference between the mean (μ) of the respective solar radiation values for SRB and BSRN. RMS is the root mean square difference between the respective SRB and BSRN values. The correlation coefficient between the SRB and BSRN values is given by ρ, the variance in the SRB values is given by σ, and N is number of SRB:BSRN month pairs for each latitude region. (Note that the solar radiation unit is kWh/day/m^2; multiplying kWh/day/m^2 by 3.6 yields MJ/day/m^2, and by 41.67 yields W/m^2.)

The statistics given in the upper left box are for all BSRN sites (Globally), those located 60-degree poleward, and for those located 60-degree equatorward. The Bias is the difference between the mean (μ) of the respective solar radiation values for SRB and BSRN. RMS is the root mean square difference between the respective SRB and BSRN values. The correlation coefficient between the SRB and BSRN values is given by ρ, the variance in the SRB values is given by σ, and N is number of SRB:BSRN month pairs for each latitude region.

(Return to Content)

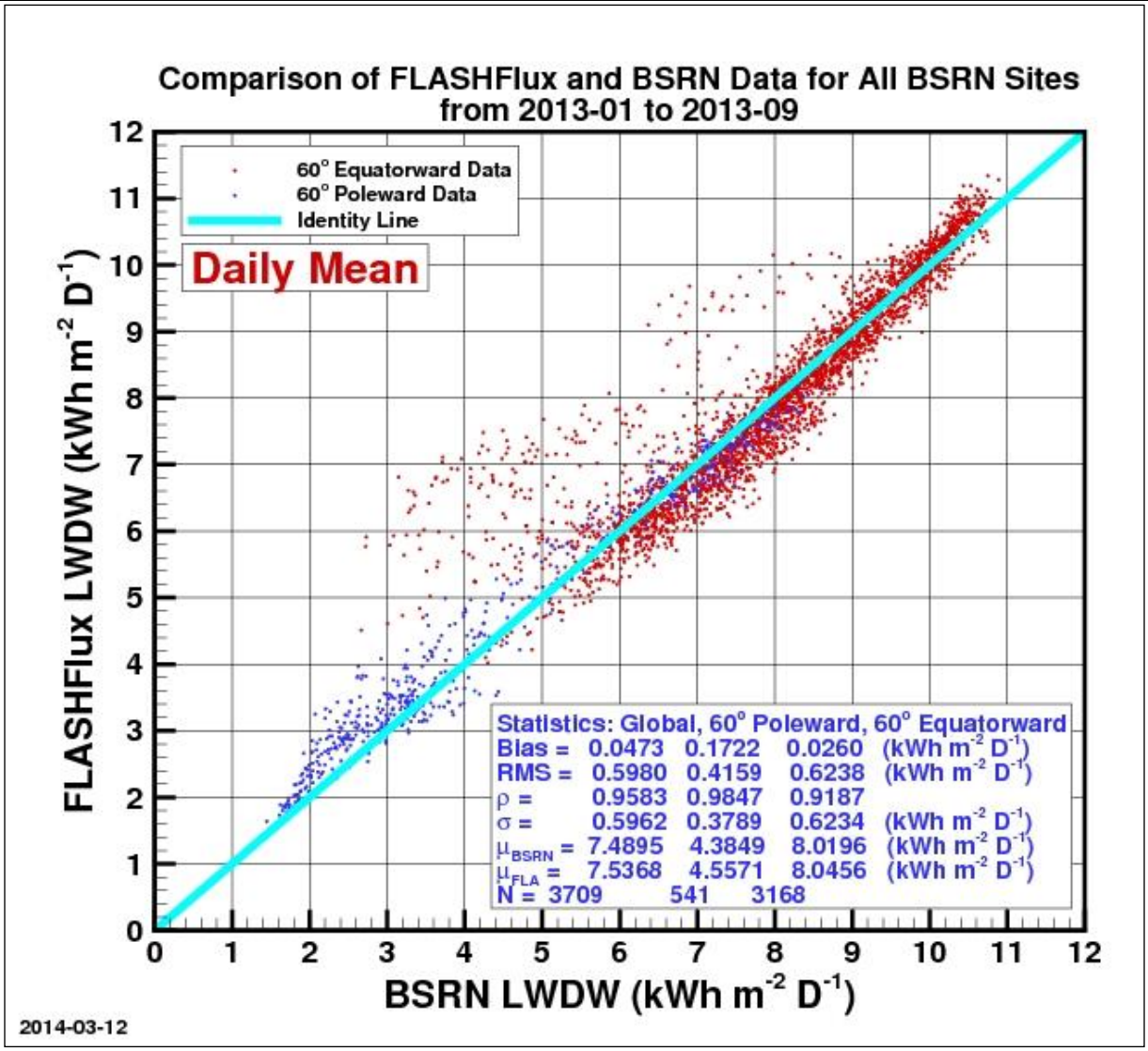

Figure 4.3.2.2.2. Scatter plot of daily total surface solar longwave radiation observed at BSRN ground sites over the years January 1, 2013 – September 30, 2013 versus daily values from the FLASHFlux version 3A. The statistics given in the upper left box are for all BSRN sites (Globally), those located 60-degree poleward, and for those located 60-degree equatorward. The Bias is the difference between the mean (μ) of the respective solar radiation values for SRB and BSRN. RMS is the root mean square difference between the respective SRB and BSRN values. The correlation coefficient between the SRB and BSRN values is given by ρ, the variance in the SRB values is given by σ, and N is number of SRB:BSRN month pairs for each latitude region. (Note that the solar radiation unit is kWh/day/m^2; multiplying kWh/day/m^2 by 3.6 yields MJ/day/m^2, and by 41.67 yields W/m^2.)

(Return to Content)

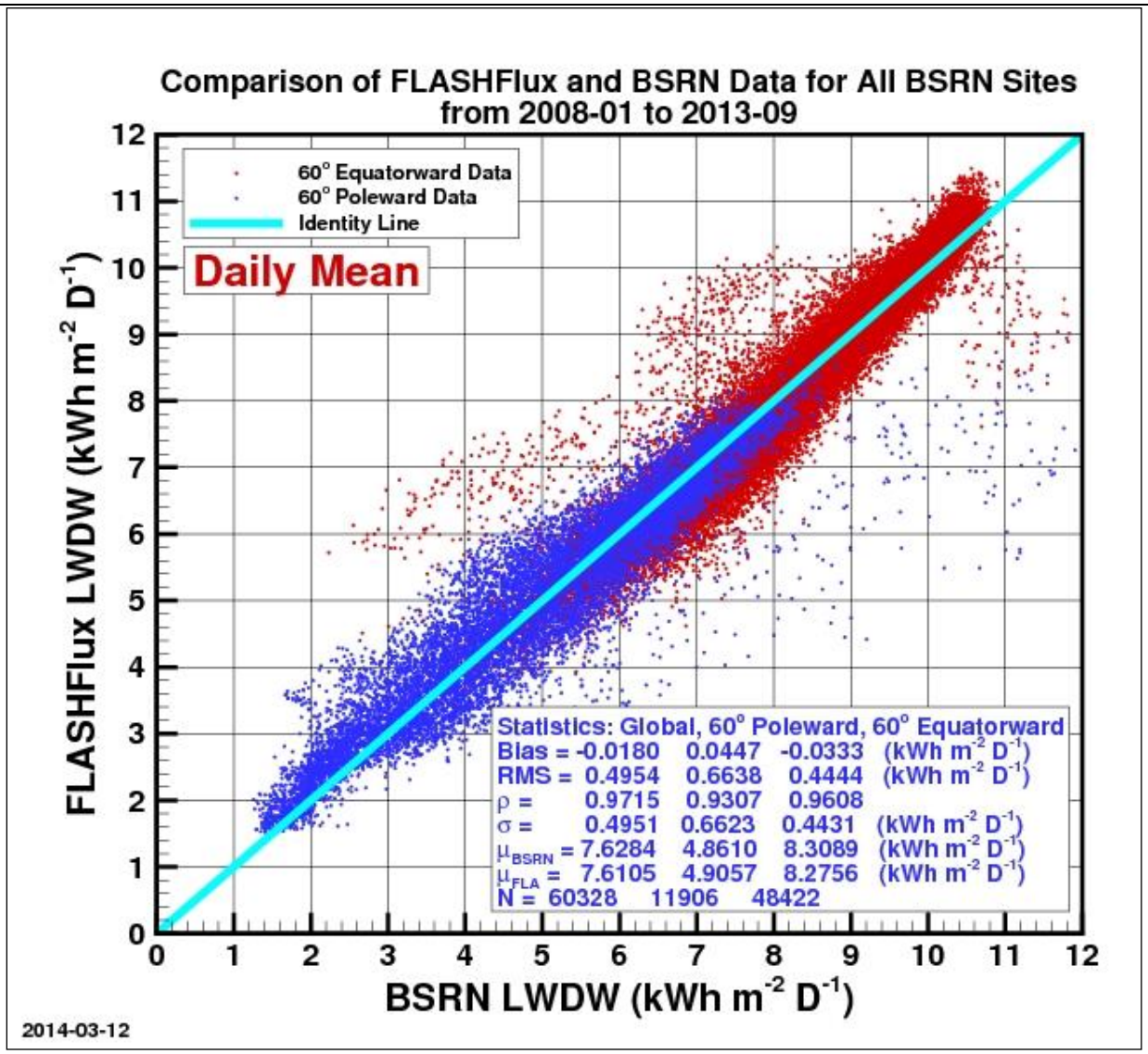

Figure 4.3.2.2.3. Scatter plot of daily total surface solar longwave radiation observed at BSRN ground sites over the years January 1, 2008 – September 30, 2013 versus daily values from the FLASHFlux version 2H+3A. The statistics given in the upper left box are for all BSRN sites (Globally), those located 60-degree poleward, and for those located 60-degree equatorward. The Bias is the difference between the mean (μ) of the respective solar radiation values for SRB and BSRN. RMS is the root mean square difference between the respective SRB and BSRN values. The correlation coefficient between the SRB and BSRN values is given by ρ, the variance in the SRB values is given by σ, and N is number of SRB:BSRN month pairs for each latitude region. (Note that the solar radiation unit is kWh/day/m^2; multiplying kWh/day/m^2 by 3.6 yields MJ/day/m^2, and by 41.67 yields W/m^2.)

(Return to Content)

5. Meteorological Parameters

The meteorological parameters available through the POWER/Sustainable Buildings Archive include:

(1) Daily mean temperature
(2) Daily maximum and minimum temperatures
(3) Surface Pressure
(4) Wind speed
(5) Specific Humidity
(6) Relative humidity
(7) Dew/frost point temperatures
(8) Precipitation
(9) Heating/Cooling Degree Days
(10) Climate Type (Briggs, et. al. 2002: Dry, Humid, Marine)
(11) Climate Zone (Briggs, et.al. 2002:1-8)

Each of these parameters is either obtained directly from or calculated using meteorological parameters taken from NASA's Modern Era Retro-analysis for Research and Applications – (MERRA) assimilation model (http://gmao.gsfc.nasa.gov/merra/) and the GEOS-5 Forward Processing for Instrument Teams (FP-IT) assimilation model. Both MERRA and FP-IT are major new versions of NASA's Goddard Earth Observing System Data Assimilation System Version 5 [GEOS-5; Rienecker et al. (2008, 2011) and Molod et al. (2011)]. Values from each model are initially produced on a 1/2-degree by 2/3-degree global grid and then bi-linearly interpolated by the POWER project to a global 0.5^{o} grid. The archive data parameters are also transformed from Universal Time (UT) to solar local time (i.e., noon is defined to be solar noon without local time zone definitions taken into account). The MERRA meteorological data encompasses the time period from January 1, 1981 through approximately three months before current time; the values from the FP-IT assimilation model is appended to the MERRA data stream for the current time minus approximately three months through a few days before current time. Accordingly the combined meteorological time series spans the time period from 1981 through several day before current time. These models are identical at the core and therefore discontinuities as a result of concatenation of the data products should be minimal.

The meteorological parameters emerging from the GMAO assimilation models are estimated via "An atmospheric analysis performed within a data assimilation context [that] seeks to combine in some "optimal" fashion the information from irregularly distributed atmospheric observations with a model state obtained from a forecast initialized from a previous analysis" (Bloom, et al., 2005). The model seeks to assimilate and optimize observational data and model estimates of atmospheric variables. Types of observations used in the analysis include (1) land surface observations of surface pressure; (2) ocean surface observations of sea level pressure and winds; (3) sea level winds inferred from backscatter returns from space-borne radars; (4) conventional upper-air data from rawinsondes (e.g., height, temperature, wind and moisture); (5) additional sources of upper-air data include drop sondes, pilot balloons, and aircraft winds; and (6) remotely sensed information from satellites (e.g., height and moisture profiles, total perceptible water, and single level cloud motion vector winds obtained from geostationary satellite images).

Emerging from MERRA are hourly global estimates of the vertical distribution of a range of atmospheric parameters.

All of the MERRA parameters represent the average value over the half-degree spatial grid. The wind speed is at 10m above the average elevation of the half-degree grid and precipitation surface value averaged over the grid. The remaining parameters are taken from the model at 2m above the average elevation of the grid box. As noted in the preceding paragraph the MERRA parameters are calculated on hourly increments. With the exception of the daily maximum and minimum temperatures the parameters enumerated above represent the daily mean in local time. The daily maximum and minimum temperatures are obtained from the 24 hourly temperature values and provided in local time.

(Return to Content)

5.1. Assessment of Assimilation Modeled Temperatures: In this section results of comparing the MERRA daily minimum and maximum temperatures, and the daily mean temperature (Tmin, Tmax and Tave) to observations reported in the National Center for Environmental Information (NCEI – formally National Climatic Data Center) global "Summary of the Day" (GSOD - http://www.ncdc.noaa.gov/oa/ncdc.html) files are presented.

The observational data reported in the NCEI GSOD files are hourly observations from globally distributed ground stations with observations typically beginning at 0Z. For the analysis reported herein, the daily Tmin, Tmax and Tave were derived from the hourly observations filtered by an "85%" selection criteria applied to the observations reported for each station. Namely, only data from NCEI stations reporting 85% or greater of the possible 1-hourly observations per day and 85% or greater of the possible days per month were used to determine the daily Tmin, Tmax, and Tave included in comparisons with the MERRA derived data.

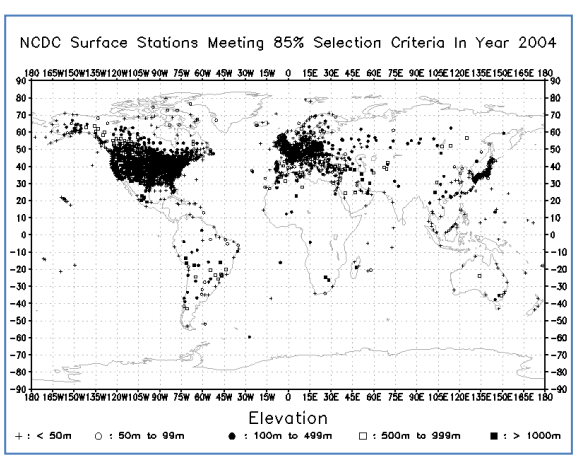

(a)

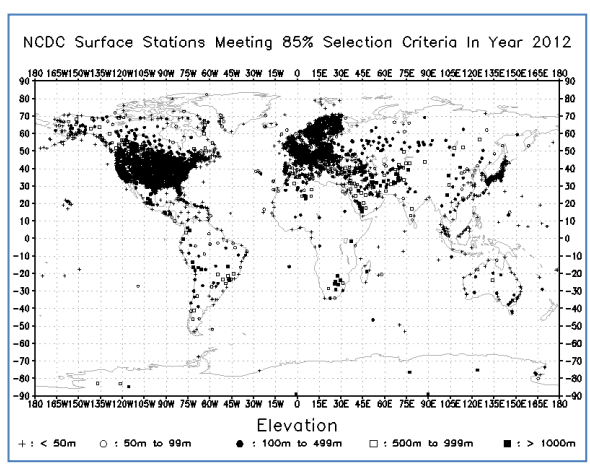

(b)

Figure 5.1.1: Figures (a) and (b) show distribution of NCEI stations meeting 85% selection criteria for 2004 and 2012, respectively.

Figure 5.1.1 shows the global distribution of the surface stations in the NCEI data files for 2004 and 2012 after applying our 85% selection criteria. There are 2704 surface stations in 2004 and 4731 in 2012 with the majority located in the northern hemisphere. As noted above, the MERRA temperatures represent the average value on a $1/2^o$ x $1/2^o$ latitude, longitude grid cell at an elevation of 2 m above the earth's surface while the NCEI values are local observations at an elevation of 2 meters above the earth's surface.

The statistical parameters used as a measure of agreement between the model estimates and surface observations are the slope, intercept and Pearson correlation coefficient associated with a linear least squares regression fit to the model vs. observational data, and the Mean Bias Error (MBE) and Root Mean Square Error (RMSE) between the model estimates and surface observations. The MBE and RMSE are given as:

(5.5.1) MBE for all stations = $\sum_j (\text{Bias})_j /(N_{stn})$,

(5.5.2) RMSE for all stations = $\sum_j (\text{RMSE})_j/ (N_{stn})$.

where,

- $(\text{Bias})_j$ = Bias for each station j = $\{\sum_i [(T_i^j)_{MERRA} - (T_i^j)_{NCEI}]\}/(N)$,
- $(\text{RMSE})_j$ = RMSE for each station j = $\{\sum_i\{[(T_i^j)_{MERRA} - (T_i^j)_{NCEI}]^2/N\}\}^{1/2}$,
- (N_{stn}) = Number of stations,
- $\sum_i$ is summation over all days meeting the 85% selection criteria,
- $(T_i^j)_{NCEI}$ is the temperature on day i for station j,
- $(T_i^j)_{MERRA}$ is the MERRA temperature corresponding to the overlapping MERRA 1/2-degree cell for day i and station j, and
- N is the number of matching pairs of NCEI and MERRA values.

The final expressions for the mean Bias and RMSE are

(5.1.3) MBE all stations = $\sum_j (\text{Bias})_j /(N_{stn})$
$= \sum_j\{\sum_i\{[(T_i^j)_{MERRA} - (T_i^j)_{NCEI}]\}\}/(\text{Nstn})$

(5.1.4) RMSE all stations = $\sum_j (\text{RMSE})_j/ (N_{stn})$
$= \{\sum_j \{\sum_i\{[(T_i^j)_{MERRA} - (T_i^j)_{NCEI}]^2/N\}\}^{1/2}\}/(\text{Nstn})$,

Figure 5.1.2 show the time series of the yearly Bias and RMSE (eqs. 5.1.3 & 5.1.4) along with the , Slope, and Pearson correlation coefficient associated with scatter plots of the MERRA daily

Tave, daily Tmin and daily Tmax vs the corresponding values from the NCEI GSOD file for each year from 1981 – 2012.

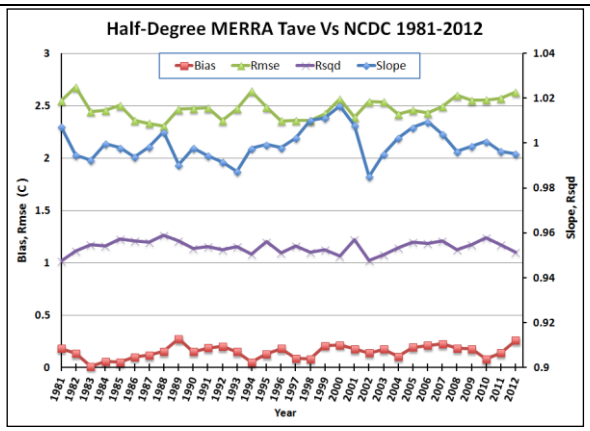

(a)

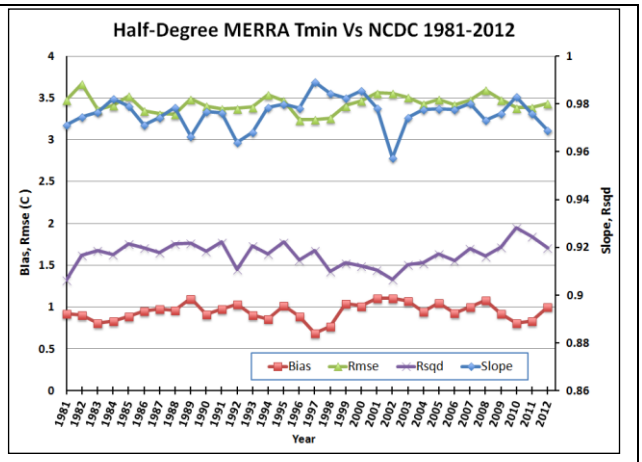

(b)

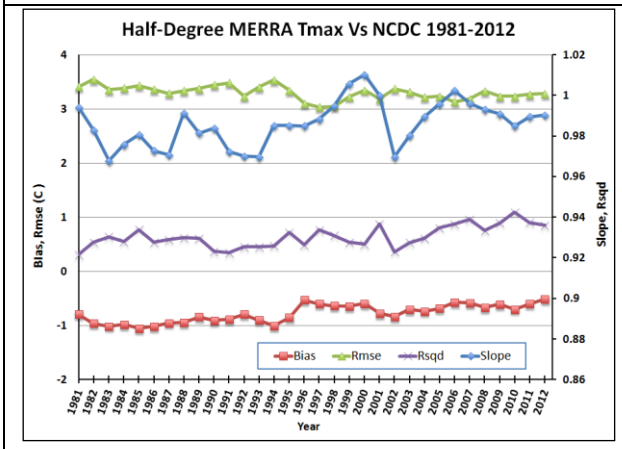

(c)

Figure 5.1.2. Time series of the yearly Bias and RMSE defined in equations (5.1.3) and (5.1.4) along with the , Slope, and Pearson correlation coefficient associated with scatter plots of the MERRA (a) daily Tave, (b) daily Tmin, and (c) daily Tmax vs the corresponding values from the NCEI GSOD file for each year from 1981 – 2012.

Table 5.1.1 lists statistical parameters associated with comparison of the MERRA half-degree daily averaged temperature (Tave) and the daily the daily minimum (Tmin) and daily maximum (Tmax) with the corresponding values taken from the NCEI GSOD file. Listed in the table are the Bias and RMSE as defined above and the slope, intercept, and Pearson correlation coefficient associated with scatter plots of MERRA and NCEI temperatures over the years 1981-2012 and corresponding scatter plots for each month in the years 1981-2012.

Table 5.1.1. Comparison statistics between MERRA temperatures and surface observations.

All years 1981 - 2012									
Parm	**Years**	**Bias**	**Rmse**	**Slope**	**Intercept**	**Rsqrd**	**TotNoP**	**AvgNoP**	**NoOfStns**
Tave	81'-12'	0.161	2.500	1.000	0.164	0.954	24262511	365	66564
Tmin	81'-12'	0.953	3.441	0.976	1.112	0.918	24255391	364	66564
Tmax	81'-12'	-0.719	3.281	0.988	-0.521	0.933	24248836	364	66564
All January months in years 1981 - 2012									
Parm	**Years**	**Bias**	**Rmse**	**Slope**	**Intercept**	**Rsqrd**	**TotNoP**	**AvgNoP**	**NoOfStns**
Tave	81'-12'	-0.317	3.047	0.990	-0.302	0.936	2057647	31	66564
Tmin	81'-12'	0.536	4.100	0.977	0.476	0.895	2056854	31	66564
Tmax	81'-12'	-1.227	3.534	0.976	-1.079	0.926	2055310	31	66564
All February months in years 1981 - 2012									
Parm	**Years**	**Bias**	**Rmse**	**Slope**	**Intercept**	**Rsqrd**	**TotNoP**	**AvgNoP**	**NoOfStns**
Tave	81'-12'	-0.243	2.797	0.980	-0.191	0.942	1878617	28	66564
Tmin	81'-12'	0.546	3.907	0.960	0.470	0.898	1878139	28	66564
Tmax	81'-12'	-1.080	3.388	0.972	-0.871	0.926	1876654	28	66564
All March months in years 1981 - 2012									
Parm	**Years**	**Bias**	**Rmse**	**Slope**	**Intercept**	**Rsqrd**	**TotNoP**	**AvgNoP**	**NoOfStns**
Tave	81'-12'	-0.117	2.552	0.966	0.096	0.939	2060849	31	66564
Tmin	81'-12'	0.604	3.535	0.941	0.691	0.894	2060319	31	66564
Tmax	81'-12'	-0.888	3.398	0.961	-0.430	0.910	2059283	31	66564
All April months in years 1981 - 2012									
Parm	**Years**	**Bias**	**Rmse**	**Slope**	**Intercept**	**Rsqrd**	**TotNoP**	**AvgNoP**	**NoOfStns**
Tave	81'-12'	0.095	2.391	0.951	0.623	0.923	1994397	30	66564
Tmin	81'-12'	0.783	3.237	0.922	1.209	0.873	1993969	30	66564
Tmax	81'-12'	-0.704	3.372	0.940	0.298	0.879	1993364	30	66564
All May months in years 1981 - 2012									
Parm	**Years**	**Bias**	**Rmse**	**Slope**	**Intercept**	**Rsqrd**	**TotNoP**	**AvgNoP**	**NoOfStns**
Tave	81'-12'	0.333	2.296	0.936	1.304	0.909	2060870	31	66564
Tmin	81'-12'	0.961	3.071	0.909	1.852	0.855	2060334	31	66564
Tmax	81'-12'	-0.501	3.272	0.915	1.278	0.852	2060274	31	66564
All June months in years 1981 - 2012									
Parm	**Years**	**Bias**	**Rmse**	**Slope**	**Intercept**	**Rsqrd**	**TotNoP**	**AvgNoP**	**NoOfStns**
Tave	81'-12'	0.437	2.277	0.924	1.873	0.896	1993757	30	66564
Tmin	81'-12'	1.047	2.972	0.898	2.434	0.840	1993133	30	66564
Tmax	81'-12'	-0.479	3.286	0.900	1.977	0.831	1993339	30	66564

Table 5.1.1. (concl'd) Comparison statistics between MERRA and Surface Observations.

All July months in years 1981 - 2012									
Parm	**Years**	**Bias**	**Rmse**	**Slope**	**Intercept**	**Rsqrd**	**TotNoP**	**AvgNoP**	**NoOfStns**
Tave	81'-12'	0.562	2.317	0.920	2.266	0.881	2060190	31	66564
Tmin	81'-12'	1.201	2.961	0.885	3.041	0.829	2059505	31	66564
Tmax	81'-12'	-0.374	3.336	0.899	2.339	0.808	2059861	31	66564
All August months in years 1981 - 2012									
Parm	Years	Bias	Rmse	Slope	Intercept	Rsqrd	TotNoP	AvgNoP	NoOfStns
Tave	81'-12'	0.643	2.307	0.928	2.145	0.888	2055316	31	66564
Tmin	81'-12'	1.382	3.073	0.883	3.205	0.836	2054715	31	66564
Tmax	81'-12'	-0.262	3.277	0.909	2.149	0.816	2054907	31	66564
All September months in years 1981 - 2012									
Parm	**Years**	**Bias**	**Rmse**	**Slope**	**Intercept**	**Rsqrd**	**TotNoP**	**AvgNoP**	**NoOfStns**
Tave	81'-12'	0.553	2.179	0.964	1.185	0.914	1992742	30	66564
Tmin	81'-12'	1.404	3.201	0.910	2.520	0.852	1992245	30	66564
Tmax	81'-12'	-0.297	3.028	0.948	0.914	0.862	1991982	30	66564
All October months in years 1981 - 2012									
Parm	**Years**	**Bias**	**Rmse**	**Slope**	**Intercept**	**Rsqrd**	**TotNoP**	**AvgNoP**	**NoOfStns**
Tave	81'-12'	0.233	2.160	0.996	0.285	0.934	2059678	31	66564
Tmin	81'-12'	1.222	3.320	0.947	1.629	0.868	2059176	31	66564
Tmax	81'-12'	-0.655	2.914	0.977	-0.252	0.903	2058596	31	66564
All November months in years 1981 - 2012									
Parm	**Years**	**Bias**	**Rmse**	**Slope**	**Intercept**	**Rsqrd**	**TotNoP**	**AvgNoP**	**NoOfStns**
Tave	81'-12'	-0.058	2.515	0.999	-0.047	0.935	1994048	30	66564
Tmin	81'-12'	0.995	3.642	0.965	1.102	0.879	1993471	30	66564
Tmax	81'-12'	-1.027	3.104	0.982	-0.812	0.921	1992692	30	66564
All December months in years 1981 - 2012									
Parm	**Years**	**Bias**	**Rmse**	**Slope**	**Intercept**	**Rsqrd**	**TotNoP**	**AvgNoP**	**NoOfStns**
Tave	81'-12'	-0.219	2.970	0.992	-0.197	0.932	2054400	31	66564
Tmin	81'-12'	0.739	4.024	0.972	0.707	0.886	2053531	31	66564
Tmax	81'-12'	-1.160	3.414	0.976	-0.985	0.923	2052574	31	66564

Figure 5.1.3 is a plot of the time series of the monthly MBE associated with Tave, Tmin, and Tmax given in Table 5.1.1 with $\pm$ boundaries (black curves) associated with the each moth's standard deviation.

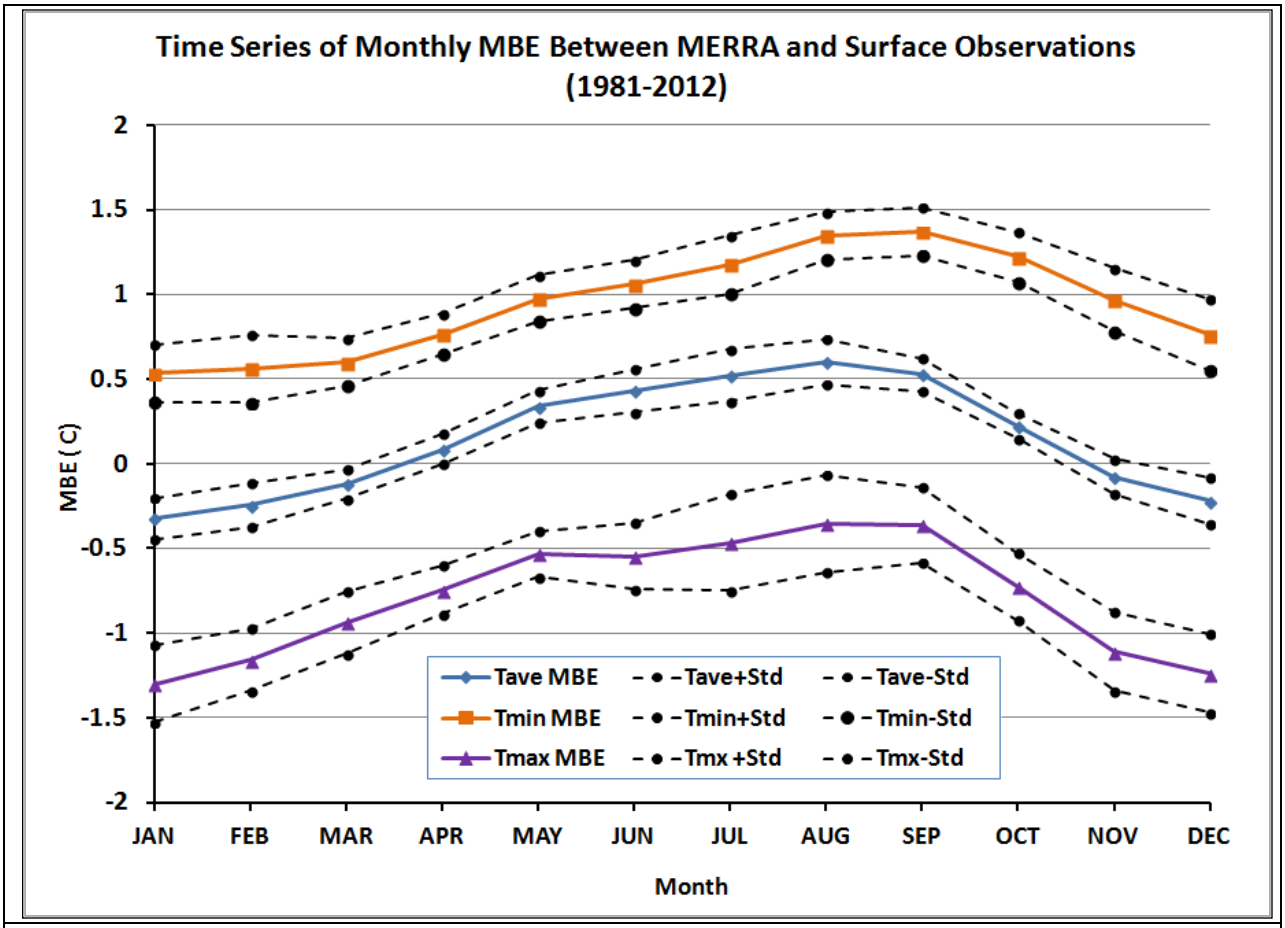

Figure 5.1.3, Time series of month bias (MBE) between MERRA daily averaged temperatures (Tave) and MERRA daily Tmin and Tmax values and the corresponding temperatures from the NCEI GSOD day files. The black dashed cures associated with the Tave, Tmin, and Tmax cures are the one standard deviation upper (plus Stdev) and lower (minus Stdev) bounds.

(Return to Content)

5.2. Relative Humidity: The relative humidity (RH) values in the POWER archives are calculated from pressure (P_a in kPa), dry bulb temperature (T_a in $^{\circ}$C), and mixing ratio (e.g. specific humidity, q in kg/kg), parameters that are available in the NASA's MERRA assimilation model. The following is a summary of the expressions used to calculate RH. The units are indicated in square brackets.

From Iribarne and Godson (1981) a fundamental definition of the Relative Humidity (Eq. 83, pg 75):

(5.2.1) $$RH = (e_a/e_{sat}) \times 100\%$$

where

e_a = the water vapor pressure and

e_{sat} the saturation water vapor pressure at the ambient temperature Ta.

The 100% has been added to cast RH in terms of percent.

Since water vapor and dry air (a mixture of inert gases) can be treated as ideal gases, it can be shown that (Iribarne and Godson, pg 74, Eq. 76; Note that the symbol, r, use in Eq. 76 for the mixing ratio has been replaced by "w" and the factor of "10" has been added to convert the units to hPa.)

(5.2.2) $e_a = (10 \times P_a \times w)/(\varepsilon + w)$ [hPa]

where w is the mixing ratio define as the ratio of mass of water to dry air and

(5.2.3) $\epsilon = \frac{R'}{R_v} = \frac{287.05}{461.5} \simeq 0.622$

where R' and R_v are the dry and water vapor gas constants respectively (note that there is no exact consensus for the gas constants past 3 significant digits, therefore the value of the ratio is kept to 3 significant digits). The mixing ratio is related to specific humidity by the relation (Jupp 2003, pg.37):

(5.2.4) $w = q / (1-q)$ [kg/kg]

Combining (5.2.2) and (5.2.4) leads to the following expression for e in terms of q:

(5.2.5) $e_a = q \times 10 \times P_a/[\varepsilon + q \times (1- \varepsilon)]$ [hPa]

An eighth-order polynomial fit (Flatau, et. al. 1992) to measurements of vapor pressure over ice and over water provides an expression to calculate the saturated water vapor pressure over ice and over water. The eight-order fit for e_{satw} is given by

(5.2.6) $e_{wsat} = A_{1w} + A_{2w} \times (T_a) + \ldots + A_{(n-1)w} \times (T_a)^n$

and

(5.2.7) $e_{isat} = A_{1i} + A_{2i} \times (T_a) + \ldots + A_{(n-1)i} \times (T_a)^n$,

Where

e_{wsat} = saturated vapor pressure over water in [hPa = mb]

e_{isat} = saturated vapor pressure over ice [hPa=mb]

T_a is the ambient dry bulb temperature in ^oC.

Table 5.2.1 gives the coefficients for e_{sat} over water and over ice and the temperature range over which the coefficient are applicable.

Table 5.2.1. Coefficients of the eight-order polynomial fit (Taken from Flatau, et. al. 1992 Table 4.) to measurements of saturated vapor pressure measurements,	
Coefficients for e_{sat} over water valid over the temperature range -85 ^oC to +70 ^oC	Coefficients for e_{sat} over ice valid over the temperature range -90 ^oC to 0 ^oC
A1w = 6.11583699	A1i = 6.09868993
A2w = 0.444606896	A2i = 0.499320233
A3w = 0.143177157E-1	A3i = 0.184672631E-1
A4w = 0.264224321E-3	A4i = 0.402737184E-3
A5w = 0.299291081E-5	A5i = 0.565392987E-5
A6w = 0.203154182E-7	A6i = 0.521693933E-7
A7w = 0.702620698E-10	A7i = 0.307839583E-9
A8w = 0.379534310E-13	A8i = 0.105758160E-11
A9w = -0.321582393E-15	A9i = 0.161444444E-14

Note that only the relative humidity over water is calculated and provided in the POWER/Sustainable Buildings Archive consistent with the values reported by the National Weather Service. Table 5.2.2 summarizes the yearly averaged comparison statistics for the relative humidity over water calculated using the formulation described above with equation 5.2.6 for the saturated water vapor over water and MERRA q, P, T values vs. the corresponding relative humidity calculated using parameters taken from the NCEI GSOD files over the years 1981-2012. Note that the Bias and RMSE (left axis) are in percentage error relative to the NCEI values. Figure 5.2.1 is a yearly time series plot of the MBE and RMSE (right vertical axis) and the slope and R^2 (left axis) associated with a linear least squares fit to the MERRA vs. NCEI scatter plot for each year between 1981 and 2012.

Table 5.2.2. Summary of statistics for a global comparison of the MERRA daily relative humidity to ground observations reported in the NCEI GSOD files during from 1981 – 2012. RH calculated using 8th order Flatau fit

Time Period	MBE(%)	RMSE(%)	Slope	Intercept	R^2	Daily Values
All Years	2.86	12.07	0.82	15.52	0.60	23,329,003
Jan	6.36	13.39	0.68	29.95	0.50	1,975,441
Feb	6.81	13.87	0.68	30.19	0.49	1,805,030
Mar	6.48	14.05	0.70	27.39	0.51	1,981,589
Apr	4.70	12.61	0.73	22.21	0.58	1,918,668
May	2.28	11.18	0.78	16.82	0.64	1,982,642
Jun	0.73	10.95	0.85	11.06	0.65	1,917,958
Jul	-0.55	11.49	0.89	6.82	0.64	1,981,827
Aug	-1.46	11.49	0.91	4.56	0.64	1,976,993
Sep	-1.09	10.76	0.93	3.78	0.68	1,916,985
Oct	1.25	10.46	0.89	9.13	0.67	1,981,343
Nov	3.77	11.41	0.82	17.31	0.62	1,917,056
Dec	5.33	12.57	0.72	26.79	0.52	1,973,471

The surface values of RH were calculated using the NCEI station values of the 2-m air temperature and the 2-m dew point temperatures. Equation (5.2.6) (with Flatau 8th order coefficients) gives an estimate of e_{wsat} for T_a = ambient temperatures and e_a for T_a = the dew point temperature both of which are measured and available in the GSOD files.

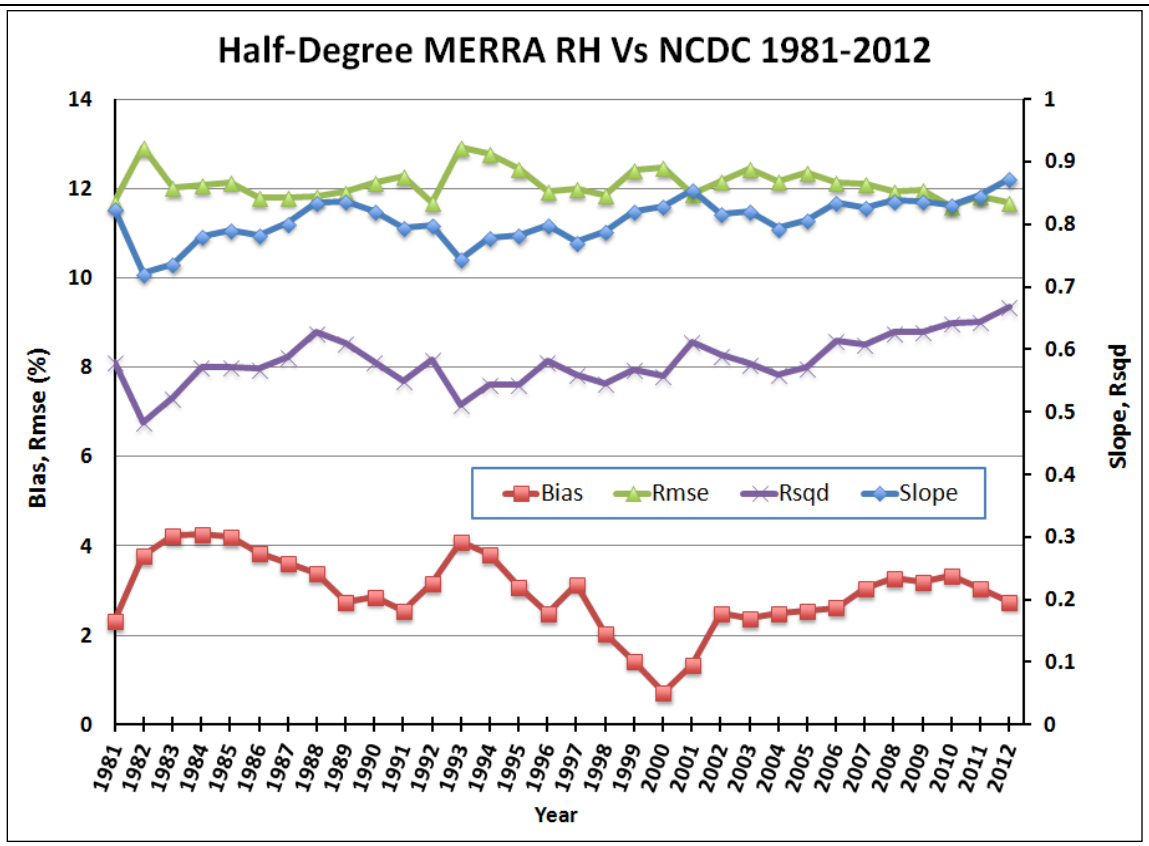

Figure 5.2.1. Statistics based upon comparison of MERRA and NCEI daily averaged relative humidity (RH) values where the daily MERRA RH values are based upon q, P, T values from the assimilation model and equations 5.2.1 – 5.2.6. NCEI RH values are calculated using observational values of the ambient and dew point temperatures.

(Return to Content)

5.3. Dew/Frost Point Temperatures: The daily dew and frost point temperatures are calculated from the relative humidity and temperature. Note that as per http://www.ofcm.gov/fmh-1/pdf/J-CH10.pdf section 10.5.1 of the "Federal Meteorological handbook N0. 1 – Surface Weather observations and Reports, September 2005", the "Dew point shall be calculated with respect to water at all temperatures." Accordingly, the nomenclature that will be used herein is to designate dew/frost point temperatures based upon the RH over water as Tdpt. The Tdpt is calculated using the expression (2003, Encyclopedia of Agricultural, Food, and Biological Engineering, Page 189, Edited by Dennis R. Heldman; Online ISBN 0-8247-0937-3).

(5.3.1) $$Tdpt = T_a - \left[(14.55 + 0.114 \times T_a) \times RH_1 + ((2.5 + 0.007 \times T_a) \times RH_1)^3 + ((15.9 + 0.117 \times T_a) \times RH_1^{14})\right]$$

Where

T_a = Ambient air temperature

and

$RH_1 = 1.0 - RH/100$.

The RH value over water is calculated, as described in Section 5.2.

Table 5.3.1 gives the climatologically averaged yearly and monthly statistics associated with comparing the MERRA based Tdpt to values calculated from upon surface observations reported in the NCEI GSOD files.

Table 5.3.1. Summary of statistics for a global comparison of the MERRA daily mean dew point to ground observations reported in the NCEI GSOD files during from 1981 – 2012. Tdpt based on RH calculated using 8th order Flatau fit

Time Period	MBE(C)	RMSE(C)	Slope	Intercept	R^2	Daily Values
All Years	0.63	2.84	0.95	0.91	0.93	23,329,003
Jan	0.79	3.40	0.95	0.64	0.92	1,975,441
Feb	0.98	3.25	0.93	0.81	0.92	1,805,030
Mar	1.14	3.07	0.90	1.19	0.92	1,981,589
Apr	1.12	2.88	0.90	1.54	0.90	1,918,668
May	0.83	2.66	0.91	1.56	0.88	1,982,642
Jun	0.51	2.50	0.95	1.11	0.87	1,917,958
Jul	0.25	2.47	0.97	0.68	0.85	1,981,827
Aug	0.10	2.47	0.99	0.22	0.86	1,976,993
Sep	0.13	2.42	1.00	0.16	0.89	1,916,985
Oct	0.38	2.54	0.98	0.52	0.90	1,981,343
Nov	0.61	2.89	0.98	0.67	0.91	1,917,056
Dec	0.71	3.30	0.96	0.66	0.91	1,973,471

The time series in Figure 5.3.1shows the yearly averaged statistics associated with comparison of daily values of the MERRA dew point with corresponding NCEI values. The statistical values are scatter plots of daily values MERRA vs NCEI for each year. Tdpt based on RH calculated using 8th order Flatau fit.

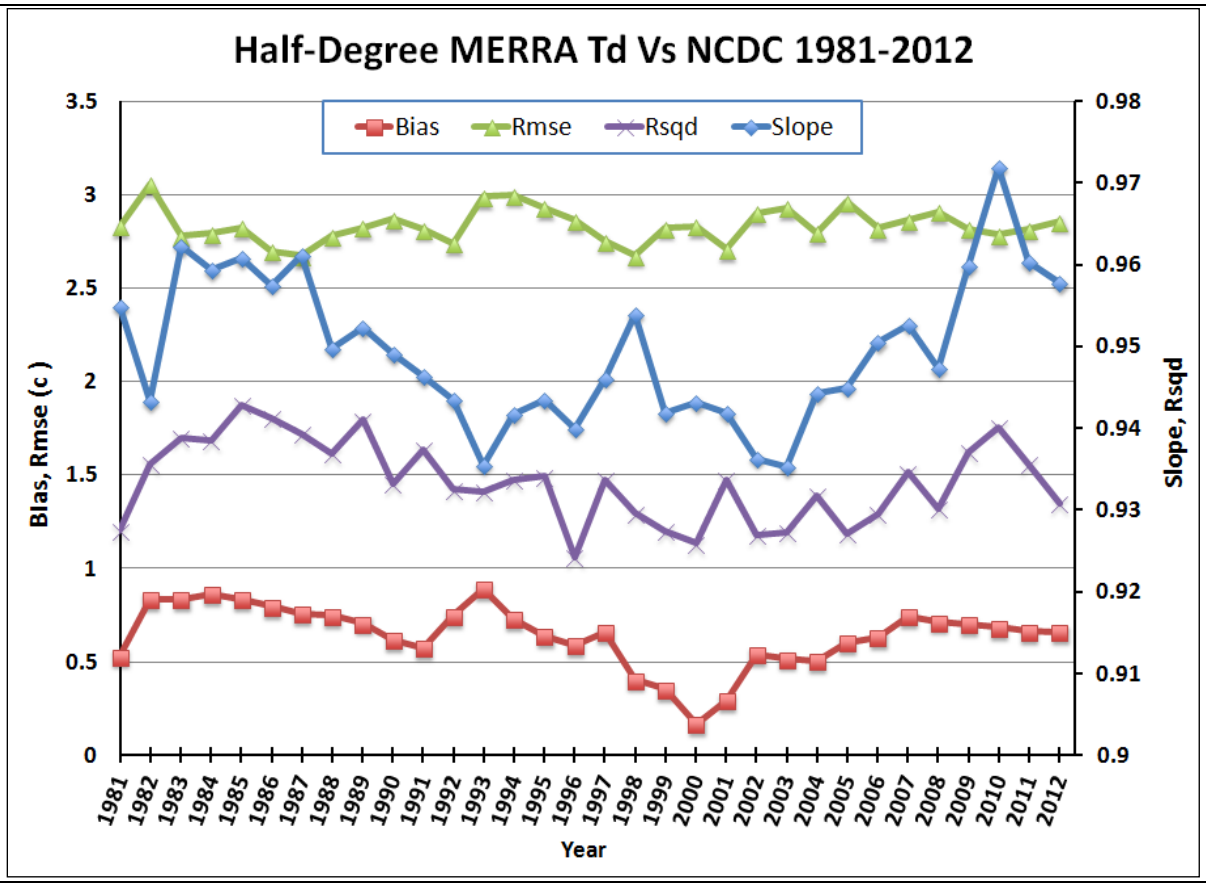

Figure 5.3.1. Yearly averaged statistics associated with comparison of daily values of the MERRA based dew point with corresponding NCEI values. The statistical values are scatter plots of daily values MERRA vs NCEI for each year. Tdpt based on RH calculated using 8th order Flatau fit.

(Return to Content)

5.4. Precipitation: The precipitation data in POWER/Sustainable Buildings Archive has been obtained from the MERRA assimilation model and represents an estimate of the daily mean value for the respective grid cell.

It is noted that the Tropical Rainfall Measurement Mission (TRMM - http://trmm.gsfc.nasa.gov/) is another potential source for precipitation data, however its polar orbit combined with a 0.25 - degree resolution limits the daily coverage that can be provided for a given location. Moreover the global coverage afforded by TRMM is nominally from 40N to 40S latitude. Currently the TRMM data is not included as part of the POWER/Sustainable Buildings precipitation data product.

We also note that Global climate Precipitation Project (GPCP) produces a global product with estimates of the daily precipitation on a 1-degree spatial grid. The data from the GPCP covers the time period from January 1, 1997 to within several months of current time. But since neither the temporal nor spatial coverage is compatible with the data MERRA data it has not been included in the POWER/Sustainable Buildings Archive.

5.4.1 MERRA Precipitation: "MERRA is a NASA reanalysis for the satellite era using a major new version of the Goddard Earth Observing System Data Assimilation System Version 5 (GEOS-5)." (http://gmao.gsfc.nasa.gov/research/merra/) The initial spatial resolution of the MERRA precipitation values is 1/2 degrees latitude × 2/3 degrees longitude at 1-hour time increments. In order to be compatible with POWER solar data, the MERRA precipitation is bi-linearly interpolated to a spatial resolution of 0.5^{o} latitude by 0.5^{o} longitude and averaged to give the daily average precipitation in local time.

5.4.2 Validation: The validation methodology employed here is similar to that described above for the temperature evaluation. Namely, observational data from the National Center for Environmental Information (NCEI – formally National Climatic Data Center) Global Summary Of Day (GSOD) files have been used as the ground-truth values. As with the temperature validation, only NCEI stations reporting 85% or greater of the possible 1-hourly observations per day and 85% or greater of the possible days per month provided the initial pool of surface stations. The rain values from the GSOD files were further filtered to omit data having a flag value indicating that the reported rain values may not represent a full 24 hour amount of rain and hence not an accurate daily average. And finally comparison statistics were only computed for stations reporting daily values for at least 1,825 days (i.e. approximately 5 years of daily values) although these were not necessarily consecutive calendar days. The number of station in the 1981 – 2013 time period was 1,675.

Table 5.4.2.1 gives the climatologically averaged yearly and monthly statistics associated with comparing the MERRA rain values to the surface observations.

Table 5.4.2.1. Summary of statistics for a global comparison of the MERRA daily mean rain to ground observations reported in the NCEI GSOD files from 1981 – 2012.

Time Period	MBE(C)	RMSE(C)	Slope	Intercept	R^2	Daily Values
All Years	0.23	6.99	0.24	1.71	0.15	1880321
JAN	0.27	6.11	0.27	1.51	0.14	1896878
FEB	0.27	5.92	0.27	1.45	0.14	1732982
MAR	0.30	6.17	0.28	1.53	0.15	1914949
APR	0.24	6.32	0.25	1.54	0.14	1864956
MAY	0.20	6.89	0.22	1.73	0.14	1924162
JUN	0.22	7.69	0.21	2.00	0.15	1859440
JUL	0.34	7.91	0.18	2.12	0.12	1923108
AUG	0.31	7.84	0.19	2.00	0.12	1919973
SEP	0.11	8.18	0.23	1.78	0.16	1861538
OCT	0.09	7.48	0.25	1.64	0.16	1919630
NOV	0.16	6.84	0.28	1.62	0.16	1852041
DEC	0.24	6.50	0.28	1.62	0.15	1894198

Figure 5.4.2.2.shows the yearly averaged time series of the statistics associated with comparison of daily values of the MERRA rain with respect to surface observations.

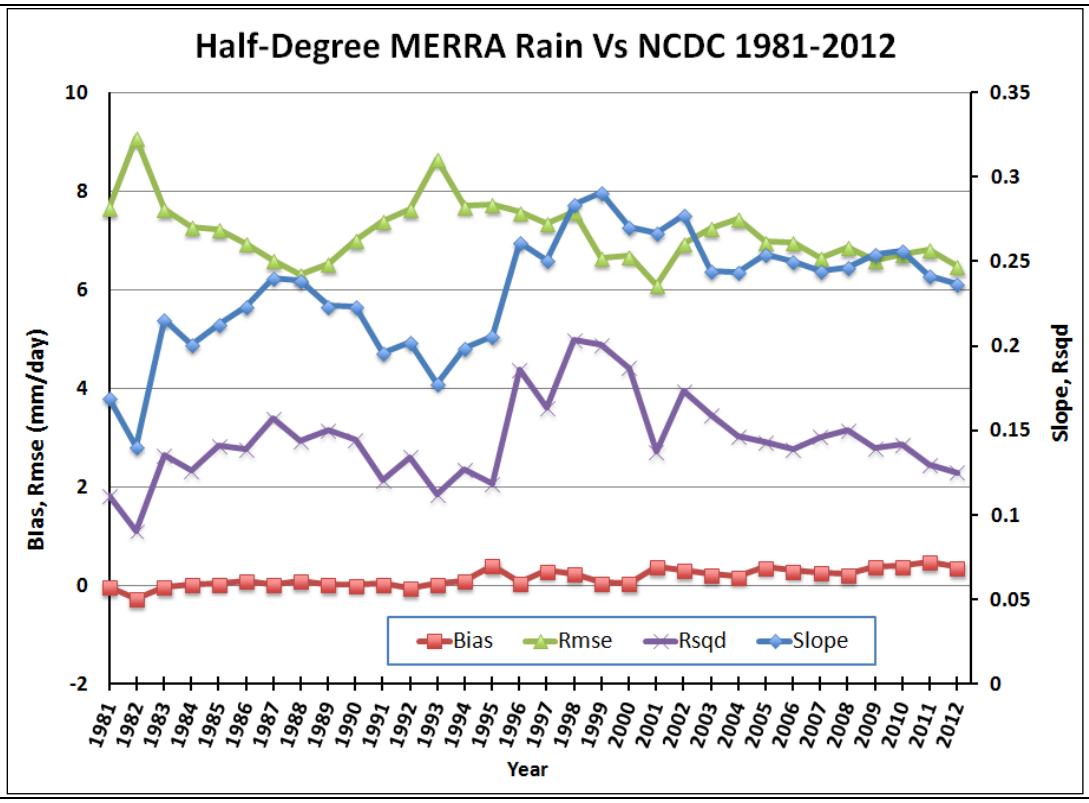

Figure 5.4.2.2. Yearly statistics associated with comparison of daily mean values of MERRA precipitation estimates to corresponding observational values reported in the NCEI GSOD files over the years 1981 – 2012. The statistical values are associated with scatter plots of daily values of MERRA vs NCEI for each year.

Just from casual observations, it is recognized that precipitation is quite often spatially non-homogeneous. Consequently, it is not unexpected that there is poor agreement between the MERRA rain values, which represent an overage over a 0.5^{o} latitude/longitude grid cell, and localized surface measurements as evident from the small slope and R^2 values shown in Table 5.4.2.1 and Figure 5.4.2.2.

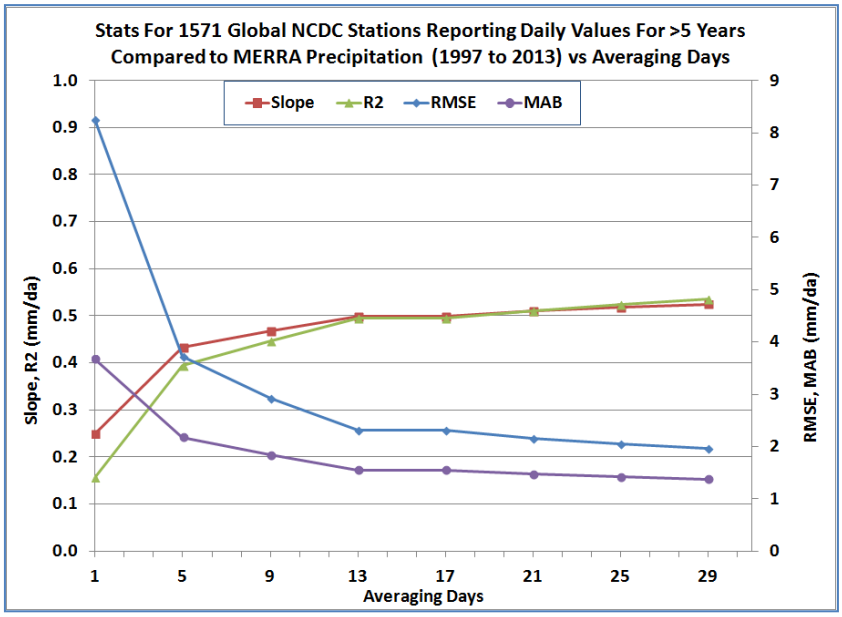

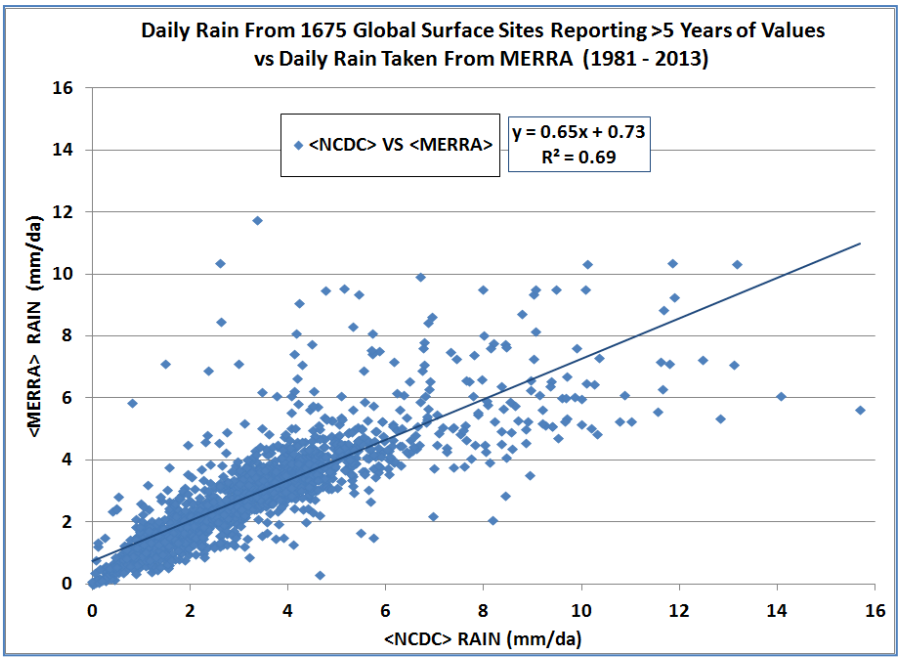

Figure 5.4.2.3.Top panel gives the dependence of the slope, R^2, RMSE, and MAB on the averaging days associated with the surface values compared to MERRA values respectively. The slope and R^2 are associated with the scatter plots of the averaged NCEI values vs. the average MERRA values. The bottom panel is a scatter plot of the long term average of the daily MERRA precipitation vs. corresponding surface values, where each symbol corresponds to the average of the precipitation over all daily values meeting the filtering criteria during the years 1981 – 2013.

Averaging the MERRA daily rain values over multiple days is expected to offer improved agreement with similarly averaged surface data. The charts in Figure 5.4.2.3 illustrate the agreement between the MERRA and measured values as a function of the days over which the rain values are averaged. The top panel gives the dependence of the slope, R^2, RMSE, and MAB on the number of days the surface observations and MERRA values are averaged. The slope and R^2 are associated with scatter plots of the NCEI values vs. the MERRA values for each averaging day value. The agreement between the surface observations and the MERRA values improves with averaging days with little additional improvement beyond about 10 days. The slope curve in the top panel suggest that after 10 days the MERRA values tend to be about 50% below the surface observations. The bottom panel of Figure 5.4.2.3 is a scatter plot of the yearly averaged MERRA values vs. corresponding yearly averaged surface measurements for each surface site.

(Return to Content)

5.5 Daily Mean Wind Speed: The daily means winds are taken from MERRA and represents estimates at 10m above the local surface over a 0.5^{o} latitude x 0.5^{o} longitude grid. Table 5.5.1 gives the yearly and monthly averaged bias, RMSE, slope, intercept, and R^2 from a comparisons of the MERRA wind data over the time period from January 1, 1981 – December 31, 2012 to observational values given in the NCEI GSOD files. The last column in the table gives the total number of daily values in the comparison. The row labeled "All Years" gives the mean values over 1981 – 2011. The row for each month gives the mean values over all the indicated months in the 1981 – 2012 time period.

Table 5.5.1 Summary of statistics for comparison of MERRA 10m daily winds to ground observations during over the time period from January 1, 1981 – 2012.

Time Period	Bias	RMSE	Slope	Intercept	R^2	Daily Values
All Years	0.36	1.74	0.65	1.64	0.48	23,944,970
Jan	0.76	2.11	0.62	2.25	0.48	2,029,843
Feb	0.66	2.00	0.63	2.11	0.49	1,853,310
Mar	0.44	1.82	0.65	1.87	0.50	2,033,488
Apr	0.22	1.64	0.65	1.59	0.49	1,967,740
May	0.06	1.52	0.65	1.36	0.48	2,033,595
Jun	0.01	1.45	0.65	1.23	0.46	1,967,738
Jul	0.04	1.42	0.64	1.23	0.44	2,033,467
Aug	0.11	1.42	0.65	1.22	0.46	2,029,520
Sep	0.29	1.56	0.66	1.43	0.50	1,967,575
Oct	0.46	1.76	0.65	1.72	0.50	2,033,185
Nov	0.60	1.94	0.62	2.03	0.48	1,968,370
Dec	0.72	2.08	0.60	2.24	0.47	2,027,139

Figure 5.5.1 shows the time series of the yearly statistics associated with comparison of daily mean values of MERRA precipitation estimates to corresponding observational values reported

in the NCEI GSOD files over the years 1981 – 2012. The statistical values are associated with scatter plots of daily values of MERRA vs NCEI for each year. Note that the average of yearly statistics plotted in Figure V.E.1 correspond to the values given in "All Years" row of Table 5.5.1.

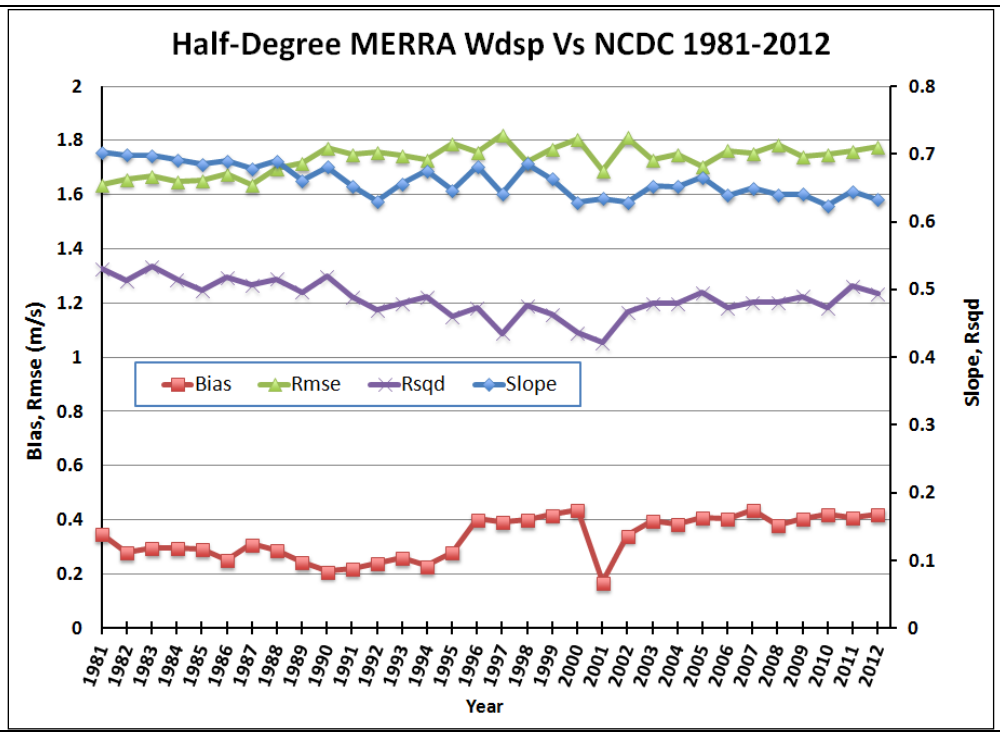

Figure 5.5.1. Yearly statistics associated with comparison of daily mean values of MERRA wind speed estimates to corresponding observational values reported in the NCEI GSOD files over the years 1981 – 2012. The statistical values are associated with scatter plots of daily values of MERRA vs. NCEI for each year.

(Return to Content)

5.6. Heating/Cooling Degree Days:

An important application of the historical temperature data is in the evaluation of Heating Degree Days (HDD) and Cooling Degree Days (CDD). The HDD and CDD are based upon the deviation of the daily averaged temperature, typically evaluated as (Tmax + Tmin)/2, relative to reference temperature, Tbase . The following give expressions used herein for calculating HDD and CDD (Chapter 14 of the ASHRAE 2009):

Heating Degree Days: For the days in a given time period (e.g. year, month, etc.)

5.6.1 $$HDD = \sum \left(T_{base} - \langle T_i \rangle\right)^+$$

Cooling Degree Days: For the days in a given time period (e.g. year, month, etc.)

5.6.2 $$CDD = \sum \left(\langle T_i \rangle - T_{base}\right)^+$$

The "+" superscript in the above equations indicates that only the positive values of the bracketed quantity are taken into account in the sum. The sum is taken from i = 1 to N, where N is number of days in the given time period.

Figure 5.6.1 illustrates the results of comparing HDD and CDD based upon MERRA

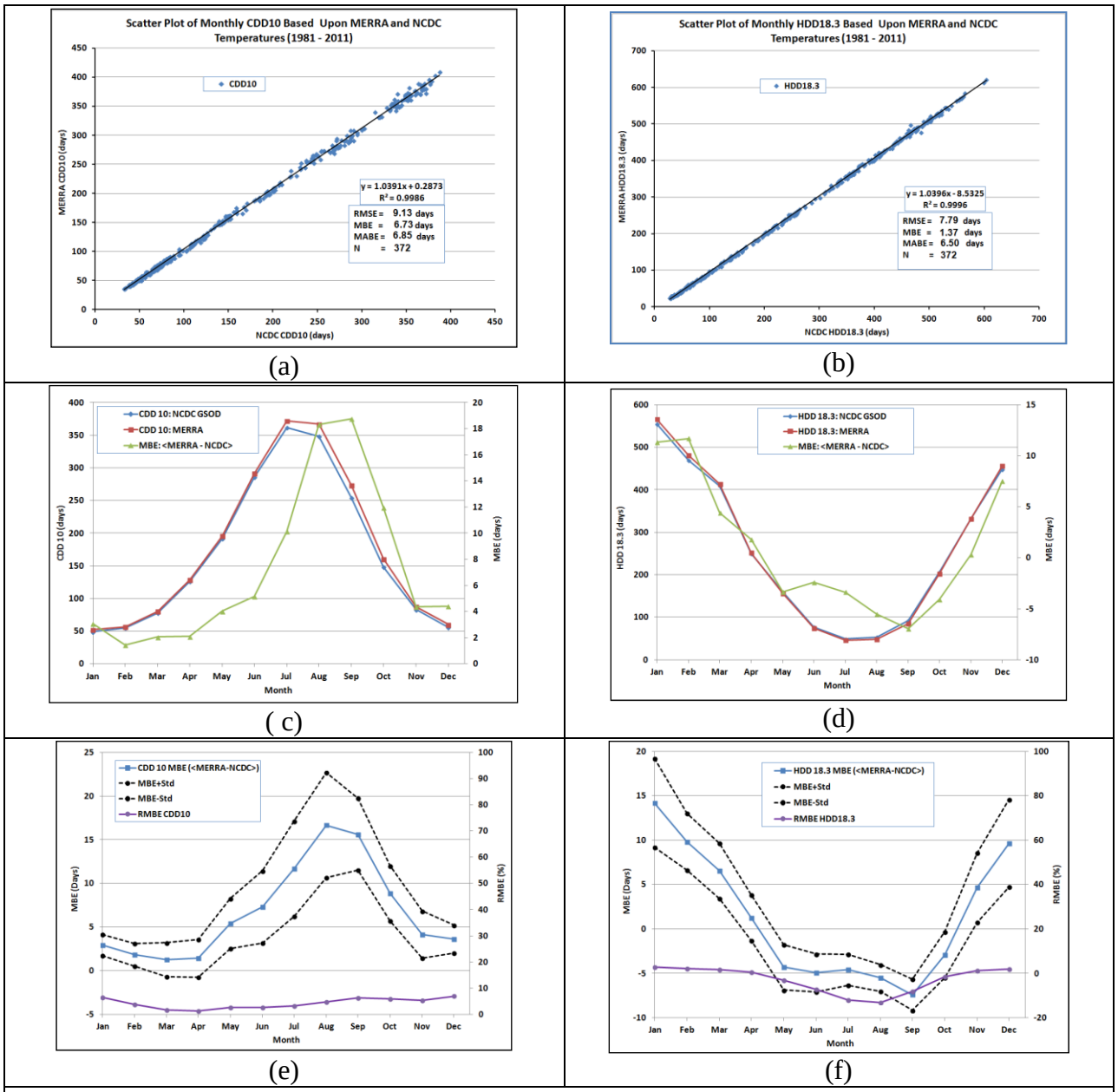

Figure 5.6.1 Results of comparing CDD (left column) and HDD (right column) values based upon MERRA and observational temperatures in the CONUS over the years 1981- 2011. Panels (a) and (b) show the scatter plot of monthly CDD10 and HDD18.3 values, respectively. Panels (c) and (d) show the monthly CDD10 and HDD18.3 values respectively and the corresponding MBE. Panels (e) and (f) show the monthly time series for the MBE (left axis) and RMBE (right axis) associated with CDD10 and HDD18.3 respectively. The dashed black curves show the $\pm$ 1-STDEV limits about the CDD and HDD MBE.

temperatures to the corresponding values based upon surface temperatures reported in the NCEI GSOD files for the CONUS over the years 1981 - 2011. The HDD and CDD values used a Tbase = 18.3°C and 10°C respectively, and the HDD and CDD values were initially evaluated as monthly values for each year. The right column shows the CDD10 results; the left column shows the HDD18.3 results. The (a) and (b) panels give the scatter plot of the MERRA vs NCDD values for all monthly CDD and HDD, respectively. Panels (c) and (d) explicitly shows the monthly MERRA and NCEI values along with the monthly mean bias error (MBE =<MERRA – MCDC>) for CDD and HDD, respectively. Panels (e) and (f) show the monthly RMSE and the monthly MBE ± std for CDD and HDD respectively, where std is the standard deviation of each months MBE over the 1981 – 2011 years.

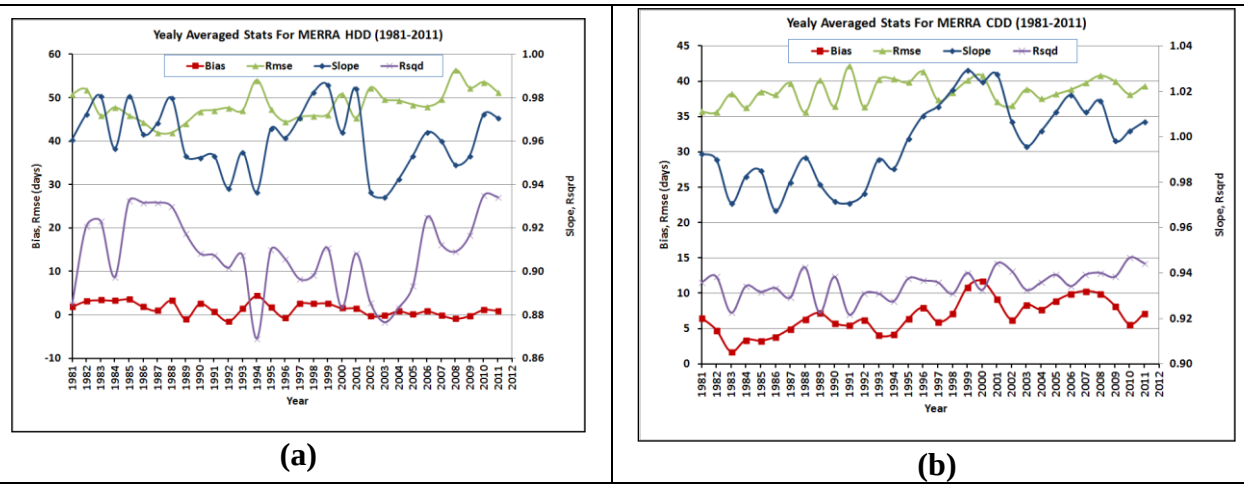

Figure 5.6.2 Yearly time series of the averaged MBE and RMSE (left vertical axis) and slope and Pearson correlation coefficient (right vertical axis) associated with linear least squares fit to MERRA vs. NCEI HDD panel, T_{base} = 18.3C (a) and CDD panel (b), T_{base} = 10.0C

(Return to Content)

5.7. Surface Pressure: The hypsometric equation (5.7.1), relates the thickness (h) between two isobaric surfaces to the mean temperature (T) of the layer as:

(5.7.1) $$h = z_1 - z_2 = (RT/g)\ln(p_1/p_2)$$

where:

z_1 and z_2 are the geometric heights at p_1 and p_2,
R = gas constant for dry air, and
g = gravitational constant.

Figure 5.7.1a shows the scatter plot of the MERRA pressure at 2-meters versus the observations reported in the NCEI archive for 2004. Figure 5.7.1b shows the improved agreement with the application of equation 5.7.1, using the 2m daily mean temperature with no correction to the MERRA temperatures (e.g. no lapse rate or offset correction). Figure 5.7.1c shows the scatter

plot where the MERRA surface pressure and temperature have been corrected for elevation differences. Clearly, adjustment to the MERRA surface pressures using equation 5.7.1 results in significant improvements to the estimates of the NCEI station pressures.

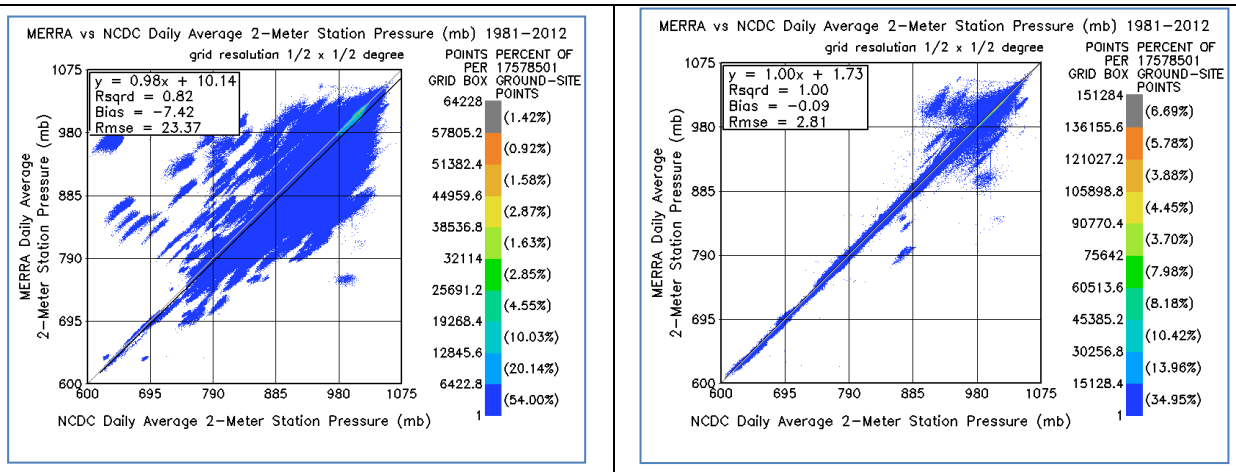

(a) (b)

Figure 5.7.1a shows the scatter plot of the MERRA pressure at 2-meters versus the observations reported in the NCEI archive from 1981 through 2012. Figure 5.7.1b shows the improved agreement with the application of equation 5.7.1 to adjust the MERRA grid cell elevation to the surface site elevation.

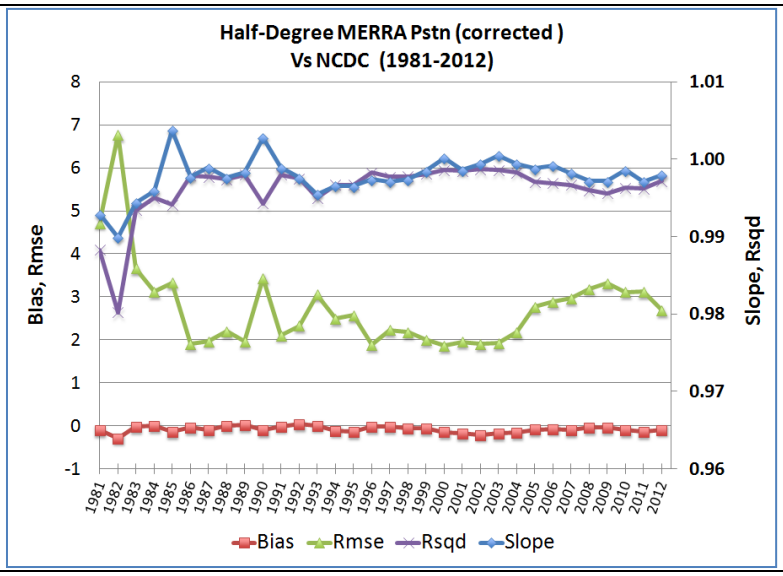

Figure 5.7.2 Time history of yearly averaged MBE and RMSE (left vertical axis) and slope and Pearson correlation coefficient (right vertical axis) associated with linear least squares fit to MERRA vs NCEI surface pressure. The stats illustrated in this figure are based upon the MERRA pressures adjusted for differences between the surface elevation and the average elevation of the MERRA ½-degree grid cell as per eq. 5.7.1.

(Return to Content)

6. References

ASHRAE. 2009a. *2009 ASHRAE Handbook – Fundamentals*. Atlanta, GA: American Society of Heating, Refrigerating and Air-Conditioning Engineers, Inc.

Bloom, S., A. da Silva, D. Dee, M. Bosilovich, J.-D. Chern, S. Pawson, S. Schubert, M. Sienkiewicz, I. Stajner, W.-W. Tan, M.-L. Wu, Documentation and Validation of the Goddard Earth Observing System (GEOS) Data Assimilation System - Version 4, Technical Report Series on Global Modeling and Data Assimilation, NASA/TM—2005–104606, Vol. 26, 2005

Encyclopedia of Agricultural, Food, and Biological Engineering edited by Dennis R. Heldman Page 189

Flatau, J. Piotr, Robert L. Walko, and William R. Cotton, 1992: *Polynomial Fits to Saturation Vapor Pressure.* Notes and Correspondence, Journal of Applies Meteorology. 1507-1513.

Gupta, S. K., D. P. Kratz, P. W. Stackhouse, Jr., and A. C. Wilber, 2001: The Langley Parameterized Shortwave Algorithm (LPSA) for Surface Radiation Budget Studies. NASA/TP-2001-211272, 31 pp. Available on-line at: http://ntrs.nasa.gov/search.jsp

Iribarne, J.V. and W.L. Godson, 1981: *Atmospheric Thermodynamics*. Geophysics and Astrophysics Monographs, D. Riedel Publishing Company, Dordrecht, Netherlands.

Jupp, D. L. B.; 2003,Calculating and converting between common water vapour measures in meteorological data and their use in support of earth observation validation, CSIRO Earth Observation Centre Technical Report, 2003/01.

Kiehl, J. T. and Kevin E. Trenberth, 1997: Earth's Annual Global Mean Energy Budget. *Bull. Amer. Meteor. Soc.*, **78**, 197–208. doi: http://dx.doi.org/10.1175/1520-0477(1997)078<0197:EAGMEB>2.0.CO;2

Molod, A., L. Takacs, M.J. Suarez, J. Bacmeister, I.S. Song, A. Eichmann, Y. Chang, 2011: The GEOS-5 Atmospheric General Circulation Model: Mean Climate and Development from MERRA to Fortuna. Technical Report Series on Global Modeling and Data Assimilation 104606 , v28

Ohmura, A., E. Dutton, B. Forgan, C. Frohlich, H. Gilgen, H. Hegne, A. Heimo, G. Konig-Langlo, B. McArthur, G. Muller, R. Philipona, C. Whitlock, K. Dehne, and M. Wild, 1998: Baseline Surface Radiation Network (BSRN/WCRP): New precision radiometery for climate change research. Bull. Amer. Meteor. Soc. 79 No. 10, 2115-2136

Pinker, R., and I. Laszlo, 1992: Modeling Surface Solar Irradiance for Satellite Applications on a Global Scale. *J. Appl. Meteor.*, 31, 194–211.

Radiation Network (BSRN/WCRP): New Precision Radiometry for Climate Research, Bull. Of American Meteor. Soc., **79**, 10, p 2115-2136.

Rasch, P. J., N. M. Mahowald, and B. E. Eaton (1997), Representations of transport, convection, and the hydrologic cycle in chemical transport models: Implications for the modeling of short-lived and soluble species, J. Geophys. Res., 102(D23), 28, 127-128, 138.

Rienecker, M.M., M.J. Suarez, R. Todling, J. Bacmeister, L. Takacs, H. C. Liu, W. Gu, M. Sienkiewicz, R.D. Koster, R. Gelaro, I. Stajner, and E. Nielsen, 2008: The GEOS-5 Data Assimilation System -Documentation of Versions 5.0.1, 5.1.0, and 5.2.0. Technical Report Series on Global Modeling and Data Assimilation 104606, V27.

Rienecker, Michele M., Max J. Suarez, Ronald Gelaro, Ricardo Todling, Julio Bacmeister,Emily Liu, Michael G. Bosilovich, Siegfried D. Schubert, Lawrence Takacs, Gi-Kong Kim, Stephen Bloom, Junye Chen, Douglas Collins, Austin Conaty, Arlindo da Silva, Wei Gu, Joanna Joiner, Randal D. Koster, Robert Lucchesi, Andrea Molod, Tommy Owens, Steven Pawson, Philip Pegion, Christopher R. Redder, Rolf Reichle, Franklin R. Robertson, Albert G. Ruddick, Meta Sienkiewicz, and Jack Woollen, 2011: MERRA: NASA's Modern-Era Retrospective Analysis for Research and Applications. *J. Climate*, **24**, 3624–3648. doi: http://dx.doi.org/10.1175/JCLI-D-11-00015.1

Rossow, W.B., and R.A. Schiffer, 1999: Advances in understanding clouds from ISCCP. *Bull. Amer. Meteorol. Soc.*, **80**, 2261-2288, doi:10.1175/1520-0477(1999)080<2261:AIUCFI>2.0.CO;2.

Smith, G.L., R. N. Green, E. Raschke, L. M. Avis, J. T. Suttles, B. A. Wielicki, and R. Davies, 1986: Inversion methods for satellite studies of the Earth's radiation budget: Development of algorithms for the ERBE mission. Rev. Geophys., 24, 407-421.

Surface Weather Observations and Reports, Federal Meteorological Handbook No. 1, FCM-H1-2005, Washington, D.C., 2005

White, Jeffrey W. , Gerrit Hoogenboom, Paul W. Wilkens, Paul W. Stackhouse Jr., and James M. Hoell, Evaluation of Satellite-Based, Modeled-Derived Daily Solar Radiation Data for the Continental United States**.** Agron. J. 103:1242-1251(2011)

(Return to Content)